Hydroxamate-Based Non-Macrocyclic Chelators for Zirconium-89 and Other Isotopes of Hard Metal Ions

by

JEFFEREY ANDREW JANG

Hons. B.Sc. University of Northern British Columbia, 2016

A THESIS SUMITTED IN PARTIAL FULFILLMENT OF
THE REQUIREMENTS FOR THE DEGREE OF

MASTER OF SCIENCE

in

THE FACULTY OF GRADUATE AND POSTDOCTORAL STUDIES

(Chemistry)

THE UNIVERSITY OF BRITISH COLUMBIA
(Vancouver)

August 2019

The following individuals certify that they have read and recommended to the Faculty of Graduate and Postdoctoral Studies for acceptance, a thesis dissertation entitled:

Hydroxamate-Based Non-Macrocyclic Chelators for ^{89}Zr and Other Isotopes of Hard Metal Ions

submitted by Jefferey Andrew Jang in partial fulfillment of the requirements for the degree of MASTER OF SCIENCE in Chemistry

Examining Committee:

Chris Orvig, Inorganic Chemistry
Supervisor

Michael Fryzuk, Inorganic Chemistry
Supervisory Committee Member

Derek Gates, Inorganic Chemistry
Supervisory Committee Member

Abstract

The development of radiopharmaceuticals for imaging and therapy has become a major focus in the field of cancer treatment. Bifunctional chelators (BFCs) attach to bioconjugates that allow for targeted radiation. This thesis examines the hydroxamate-based (hydroxamic acid) ligands for hard radiometal ions, such as zirconium-89. The current gold standard for $^{89}Zr^{4+}$ complexation is the chelating siderophore, desferrioxamine, a hexadentate ligand that has been shown to have stability issues for complexation with $^{89}Zr^{4+}$. New hydroxamate ligands have shown that flexibility is an issue for having four arms bind to $^{89}Zr^{4+}$. The potentially octadentate, hydroxamate-based ligand, H_4octaha **(1)**, was designed to overcome the flexibility issue. The synthesis of H_4octaha **(1)** encountered issues with the formation of a side reaction when synthesizing a protected arm and the selectivity of amines when alkylating the dien backbone. These issues led to the development of a new ligand, H_5decaha **(2)**. H_5decaha **(2)** is a potentially decadentate, hydroxamate-based ligand that was designed to solve the issues with the synthesis of H_4octaha **(1)**. The synthesis of the ligand was completed; however, the yield was too low for analysis by ^{1}H NMR and ^{13}C NMR. Initial complexation test for H_5decaha **(2)** with Ga^{3+} suggest that the ligand was synthesized and H_5decaha **(2)** complexes with a Ga^{3+} ion and two Na^+ ions. The ligand H_4noonha **(3)** is a potentially octadentate, hydroxamate-based ligand that uses 1,2-bis(aminoethoxylethane) as a backbone replacing dien. The ligand was synthesized and analyzed by ^{1}H NMR spectroscopy; however, due to a contaminant, additional analyses could not be completed. Additional synthesis attempts were made; however, not enough product was obtained to continue

the analysis for characterization. The functionalized dien **(4)** was synthesized to make H_4octaha **(1)** and H_5decaha **(2)** into bifunctional chelators. Purification by reduced pressure and column chromatography were not successful. The backbone was precipitated out as an HCl salt, which suffers from insolubility issues making analysis difficult.

Lay Summary

Nuclear medicine is a field of medicine that uses radiation for imaging and therapy of various diseases, such as cancer. Chelators are one of the approaches that can be used for radiometal-based pharmaceuticals. In this thesis, a group of chelators that use a chemical binding group “hydroxamate” have been explored for binding metals, such as zirconium. The goal for these ligands is to be incorporated into the toolkit for radiopharmaceuticals in clinical applications.

Preface

This dissertation is original, unpublished work by the author J. Jang. Chapter 2, Section 2.2 was developed with Dr. Sarah Spreckelmeyer, a former PhD, student in the Orvig group at the University of British Columbia. Chapter 2, Section 2.3 was developed with Dr. Xiaozhu Wang, a postdoctoral fellow in the Orvig group at the University of British Columbia.

Table of Contents

List of Tables

List of Figures

List of Schemes

List of Abbreviations

~	approximate
α	Alpha particle
β^-	Beta particle
β^+	Positron
γ	Gamma ray or photon
ν	neutrino
$\bar{\nu}$	Antielectron neutrino
δ	Delta of chemical shift in parts per million
μ	micro (10^{-6})
Δ	Heat or reflux
BFC	Bifunctional chelator
Boc_2O	Di-tert-butyl-dicarbonate
calcd.	Calculated
°C	degrees Celsius
d	Days or doublet (NMR)
dd	Doublet of doublets (NMR)
DFO	Desferrioxamine
DFO*	Desferrioxamine-star
DFT	Density functional theory (*in silico* calculations)
DMF	Dimethylformamide
DNA	Deoxyribonucleic acid
Dien	Diethylenetriamine
e^-	electron
EC	Electron capture
En	Ethylenediamine
ESI-MS	Electrospray-ionization mass spectrometry
eV	Electronvolt(s)
EtOAc	Ethyl Acetate
FSC	Fusarinine C
g	gram(s)
h	hour(s)
HOPO	1-Hydroxy-N-(3-(6-hydroxy-5-oxocyclohexa-1,3-diene-1-carboxamido)propyl)-N-(4-(1-hydroxy-N-(3-(1-hydroxy-6-oxo-1,6-dihydropyridine-2-carboxamido)propyl)-6-oxo-1,6-dihydropyridine-2-carboxamido)butyl)-6-oxo-1,6-dihydropyridine-2-carboxamide
^1H NMR	Hydrogen Nuclear Magnetic Resonance
HPLC	High Performance Liquid Chromatography
$H_4EDT(M)HA$	Ethylenediamine-tetra(methylene-N-methylhydroxamic acid)
H_4noonha	N,N,N,N-Tetra-(N-methylbutohydroxamic acid)-1,2 bis(2-aminoethoxyl ethane

H_4neunpa-NCS	N-(carbonyl)-N,N-(6-carbonylpyridine-2-yl)-N-(4-N-chlorosuccinimidephenenethyl)-1,2-triaminodiethane
H_4octaha	Diethylenetriamine-1,1,3,3-tetra(propylene-N-methylhydroxamic acid)
H_4THL	3-(N-(2-(bis(2-(hydroxy(methyl)amino)-2-oxoethyl)amino)-2-oxoethyl)-N-(4-(3-(4-isothiocyanatophenyl)thioureido) butyl)glycyl)-N1,N5-dihydroxy-N1,N5-dimethylpentanediamide
H_5decaha	Diethylenetriamine-penta(propylene-N-methylhydroxamic acid)
H_z	Hertz
IsoSiM	Isotopes for Science and Medicine
J	Coupling constant (NMR)
k	Kilo (10^3)
L	Litre(s)
LET	Linear Energy Transfer
m	Milli (10^{-3}) or meter or Multiplet (NMR)
M	Mega (10^6)
min	minute(s)
mol	moles
MS	Mass spectrometry
m/z	Mass per unit charge
n	nano or neutron
NCS	N-chlorosuccinimide
NSERC	Natural Sciences and Engineering Research Council of Canada
p	proton
PET	Positron Emission Tomography
ppm	Parts per million
q	Quartet (NMR)
RT	Room Temperature
s	Singlet (NMR)
SPECT	Single-Photon Emission Computed Tomography
t	Triplet (NMR)
T	Tesla
$t_{1/2}$	Half-life
t_R	Retention time (HPLC)
TFA	Trifluoroacetic Acid
THF	Tetrahydrofuran
THPN	1,3-Propanediamine-N,N,N',N'-tetrakis[(2-(aminomethyl)-3-hydroxy-1,6-dimethyl-4(1H)-pyridinone)acetamide]
TLC	Thin layer chromatography

Acknowledgements

First and foremost, I would like to thank my supervisor, Dr. Chris Orvig for his support and guidance throughout my degree. I would like to thank all the wonderful people in the Orvig group that I have had the chance to work with over the past 3 years. I acknowledge Dr. Sarah Spreckelmeyer, a previous PhD student in our group, who developed the original idea for an octadentate, hydroxamate-based ligand with dien backbone for the complexation with $^{89}Zr^{4+}$; Dr. Xiaozhu (Hunter) Wang, a PhD graduate, and postdoctoral fellow of the group, who has provided insight in solutions to synthesis challenges. The NSERC CREATE program, IsoSiM, at TRIUMF provided me a stipend for three years.

Chapter 1. Introduction

1.1 Radiopharmaceuticals

Nuclear medicine is an interdisciplinary field that uses radiotracers (radiopharmaceuticals) to diagnose and treat diseases. Diagnosis makes up 95% of nuclear medicine while therapy makes up the remaining 5%. Radiopharmaceuticals used in both cases can be divided into organically derived or radiometal-based.[1]

The field of radiometal ion-based pharmaceuticals has become of increasing interest in modern medicine; specifically, for targeted radiation therapy and molecular imaging.[2] One approach to radiometal ions-based pharmaceuticals is using a bifunctional chelator.

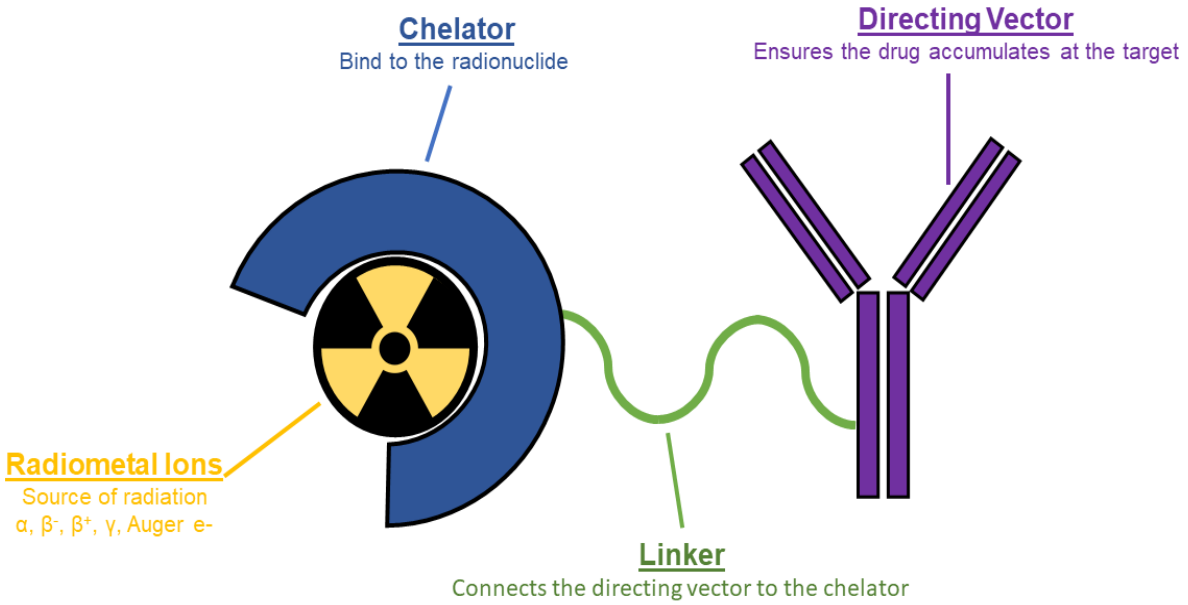

Figure 1-1. Four components of bioconjugates as target-specific radiopharmaceuticals.

There are four main components that make up bioconjugates as target-specific radiopharmaceuticals: the radiometal ion, the bifunctional chelator (BFC), the linker, and the directing vector. Radiometal ions provide a source of radiation for imaging and treatment of diseases. Chelators, which are produced through synthetic means or isolation from natural products, bind the radiometal ion to control the radiation travelling *in vivo*. The linker attaches the chelator to the directing vector and can be used to modify pharmacokinetics and pharmacodynamics. The directing vector targets specific cells by binding to membrane bound proteins on the surface of a tumor. Bioconjugates are often antibody-based, such as trastuzumab, a monoclonal antibody that targets breast cancer.[3]

A BFC has certain requirements to be suitable for clinical applications: kinetic inertness, thermodynamic stability, complexation conditions, and synthetic accessibility.[4] The thermodynamic stability and kinetic inertness of the complex reduce the likelihood of the radiometal ion being released following administration and control how fast the complex forms, respectively. Complexation conditions are important for a good pharmaceutical: near physiological pH, room temperature, and quick complexation. A pH that prevents hydroxides from forming to prevent the radiometal ion from precipitating out allows for a higher radiochemical yield. Room temperature for complexation is needed as many bioconjugates are either antibodies or small proteins which can be denatured at warmer temperatures. Quick complexation with the radiometal ion reduces the amount of radiation lost during decay. The synthesis needs to be easy and cost efficient for a new radiopharmaceutical to replace existing ones. If the synthesis is too long or difficult, the cost can increase, making the radiopharmaceutical not clinically viable.

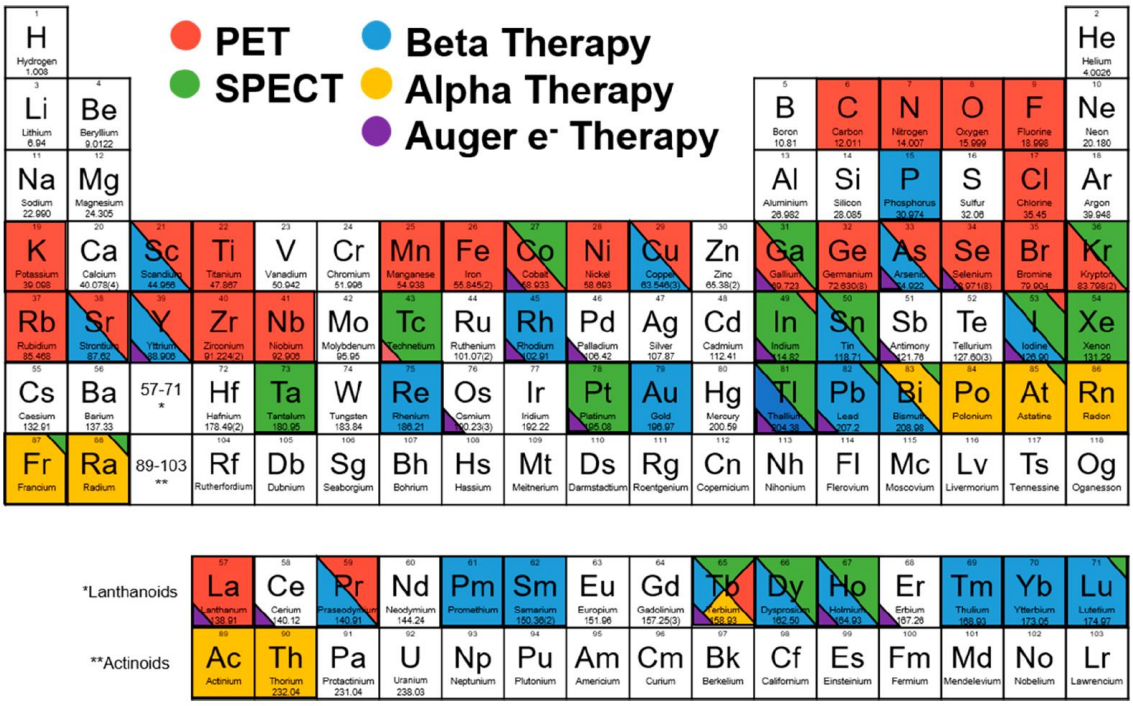

Figure 1-2. Color-coded periodic table with current or potential applications of each element in diagnostic and/or therapeutic radiopharmaceuticals.[1]

Depending on the type of decay, the radiometal ion can be used for either imaging, therapy, or both (Figure 1-2). There are five types of radiation used for radiometal ion-based pharmaceuticals: α-particles, β^- particles, β^+ particles, γ-rays, and Auger electrons. The characteristics of the five types of radiation determine whether the radiation is used for imaging and therapy (Table 1-1).

An α-particle is a helium nucleus consisting of two protons and two neutrons. Following the release of its α-emission by a radiometal, such as ^{225}Ac, a β^- particle, γ-ray, or both can be released. The α-particle released has high energy compared to other forms of radiation and a high linear energy transfer (LET), the amount of atom ionization per unit length of the path of the radiation.[1] The high LET allows for a controlled release of radiation in a small area for therapy.

Table 1-1. Types and uses of radiation in radiopharmaceuticals.[1,4]

Emission	Isotopes	Medical Application
α-particle	^{225}Ac	α-therapy
β^- particle	^{177}Lu, ^{90}Y	β^- particle
β^+ particle	^{64}Cu, ^{18}F, ^{89}Zr	PET
γ-ray	^{99m}Tc	SPECT
Auger e^-	^{67}Ga, ^{111}In	Auger e^- therapy

.

A β^- particle is produced when the nucleus of a radioactive isotope is neutron rich as is ^{177}Lu. The neutron splits into three components: a proton (p), a β^- particle (electron), and an antielectron neutrino ($\bar{\nu}$) (equation 1-1).

$$n \rightarrow p + \beta^- + \bar{\nu} \qquad \text{equation 1-1}$$

The antielectron neutrino ($\bar{\nu}$) is a subatomic particle, almost without mass and charge, used for conserving the energy for β^- decay. If the daughter from the decay is in an excited state, then a γ-ray may also be released. By interacting with the surrounding matter, the β^- particle can create another form of radiation called *bremsstrahlung*. As the β^- particle passes through the surrounding matter and is decelerated by the Coulomb field of the atomic nuclei, energy is released as X-rays called *bremsstrahlung*.[4]

A β^+ particle is produced when the nucleus of a reactive isotope is proton rich. The proton splits into three components: a neutron (n), a β^+ particle (positively charged electron), and a neutrino (ν);

$$p \rightarrow n + \beta^+ + \nu \qquad \text{equation 1-2}$$

The neutrino (ν) is a subatomic particle used for energy conservation like the antielectron neutrino ($\bar{\nu}$) for β^- decay. The positron travels through matter until it is annihilated with an electron generating two 511 keV photons that travel 180° opposed. The most common β^+ emitting isotope is ^{18}F, which is used for imaging the brain.

Auger electrons and γ-rays can be produced by electron capture or isomeric transition. In electron capture, an inner shell electron is captured by the nucleus transforming a proton into a neutron, as with ^{111}In. The vacancy in the inner shell is filled with an outer orbital electron which releases energy in the form of a γ-ray. Another possible result of electron capture is the energy released is absorbed by a different outer orbital electron ejecting it as an Auger electron.

Isomeric transitions occur when the nucleus of an isotope remains in an energy state above the ground state. The isomeric state (excited state) will decay to the ground state releasing a γ-ray. The γ-ray may be released from the isotope or it can be absorbed by an outer shell electron which is released as an Auger electron. A long-lived isomeric state is referred to as a metastable state. The most common metastable state isotope is ^{99m}Tc ($t_{1/2}$ = 6 h), an isotope of technetium used in >85% of imaging procedures around the world using single photon emission computed tomography (SPECT).

1.2 Radiotherapy

Radiotherapy uses radiation to treat various diseases and illnesses through alpha therapy, beta therapy, and Auger e^- therapy. A BFC transports the radiometal ion to the desired location where the radiation causes irreversible DNA damage that can result in deletions, chromosome aberrations, and cell death.[1] To minimize DNA damage to

surrounding healthy cells, a low energy and high LET is preferred. The low energy prevents the radiation from travelling too far from the target site and the high LET signifies a high energy deposit of radiation within the cells. These two characteristics help control the damage to cellular DNA. α-particles have high energies (5-8 MeV) as the radiation sources for therapy, along with a very high LET (~80 keV/μm). These characteristics result in a high energy transfer in a short tissue range which is ideal for treatment. β^- particles have mid-range energy (0.1-2.2 MeV) and a low LET (0.2 keV/μm) which results in a longer decay pathway that most often extends past the targeted region.[1] Auger electrons have the lowest energy (1-10 keV) and a high LET (4-26 keV/μm) resulting in the radiation distance being less than the diameter of a cell.

Two radiometal ions of interest for radiotherapeutic applications are ^{47}Sc and ^{225}Ac. ^{47}Sc ($t_{1/2}$=80.4 h) is a low energy β^- emitter used in the treatment of small tumors.[1] The production method for ^{47}Sc results in the co-production of ^{46}Sc ($t_{1/2}$=83.79 d), a β^- emitting isotope, which has made the use of ^{47}Sc less desirable for clinical application. Successful labeling with ^{44}Sc for PET imaging has brought interest for ^{47}Sc in the hopes to create a theranostic pair ^{44}Sc/^{47}Sc.[1]

^{225}Ac ($t_{1/2}$=9.91 d) is an α emitter that is viewed as one of the most promising therapeutic radiometal ions. When ^{225}Ac decays, four successive α-particles are released which can increase the effectiveness of therapy. This decay pattern combined with the long half-life, suitable for the biological half-life on many bioconjugates makes ^{225}Ac a prime candidate for targeted radiation therapy. The main concern with ^{225}Ac is its accessibility and high cost which has limited the scope of preclinical and clinical studies.

1.3 Radio-Imaging

Radiometal ions used in medicine can be divided into two groups, those used for therapy and those used for imaging. Imaging is further divided into two groups, single-photon emission computed tomography (SPECT) and positron emission tomography (PET) (Figure 1-3). SPECT is an imaging method that requires a γ-emitting radionuclide and a single detector to generate a planar image (Figure 1-3).[5,6] The half-lives of γ-emitting radionuclides such as ^{11}C, ^{18}F, and ^{89}Zr, allow for *in vivo* imaging from several hours to days.[6] SPECT systems can detect radioactive imaging compounds in concentrations below 10^{-6} M, with the resolution being affected by the photons that are attenuated or scattered. The resolution is dependent on the distance that the photon travels and can be improved by using a collimator which allows only parallel photons to hit the detector. For medical imaging, SPECT accounts for 70-80% of the scans because the cost of running a SPECT scan is much lower than running a PET scan.[5]

PET scans make use of β^+-emitting radiometal ions which release a positron (β^+), that almost immediately collides with an electron producing two 511 keV γ-rays $180^o \pm 0.25^o$ opposed which hit two detectors creating signals that can be used to generate a three-dimensional image (Figure 1-3). This method of detection allows for a higher percentage of emissions to be used in generating an image, which results in the sensitivity of PET being two or three orders of magnitude greater than for SPECT allowing the use of concentrations as low as 10^{-9} M. The resolution of PET imaging is affected by two different factors: the non-collinearity of the photon, and the range the positron travels. The non-collinearity results from the momentum of the positron and electron colliding being non-zero creating a slight deviation from the 180^o trajectories which blurs the image. The

distance a positron travels after being produced during decay affects the resolution of the image. The positron (β^+) travels through medium before it is annihilated, which can be enough to create an inaccuracy in the image. A strong magnetic field above 5 T has been shown to reduce the travel range of the positron (β^+), minimizing this effect.[6]

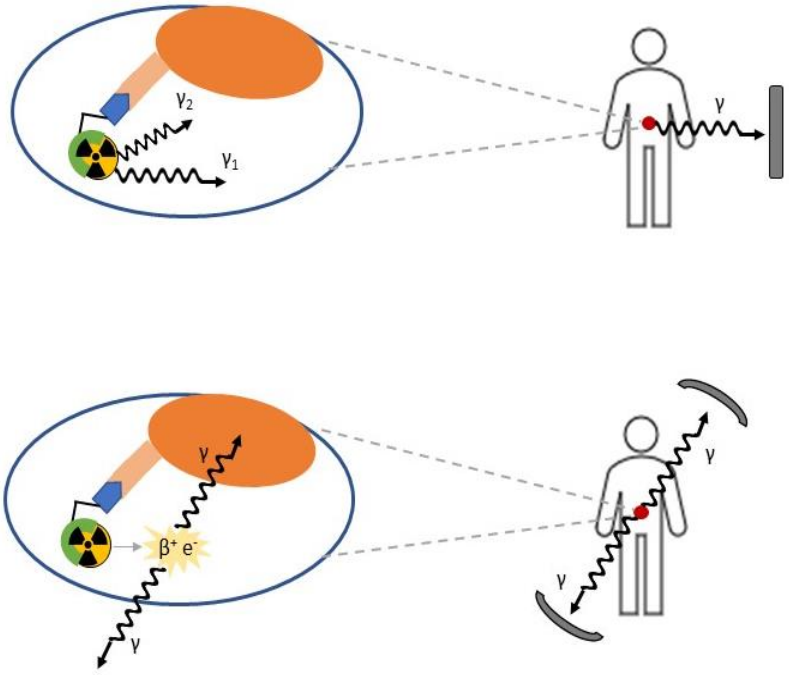

Figure 1-3. Diagram of SPECT imaging (top) and PET imaging (bottom).[5]

1.4 Radiometal Ions for Imaging

PET imaging methods use positron-emitting radionuclides including ^{11}C, ^{18}F, ^{68}Ga, ^{86}Y, ^{64}Cu, ^{124}I, and ^{89}Zr.[1,5,7] While these radionuclides have been used as sources of radiation for diagnostics, there are factors that limit their compatibility with antibody-based bioconjugates.[5] The main obstacle is the biological half-life of antibodies, which can be up to several days, much longer than many of the half-lives of these radiometal ions. The

radionuclides ^{11}C, ^{18}F, ^{64}Cu, ^{68}Ga and ^{86}Y have short half-lives that are not compatible with antibody-based bio-vectors (Table 1-2).[1,5,7] ^{124}I has a more ideal half-life, corresponding better to the biological half-life of the antibody-based bioconjugates, but has low resolution caused by the high energy positrons generated from decay. ^{89}Zr has both an ideal half-life for compatibility with antibody-based bioconjugates and positron (β^+) energies low enough to produce a high-resolution image (Table 1-2).

^{89}Zr is a positron-emitting radiometal with a long half-life of 78.4 h (Figure 1-4), making it compatible with PET imaging up to 7 days.[8–10] Zirconium is typically found in the +4-oxidation state in an aqueous environment and favours the formation of 8-coordinate complexes.[10] Zirconium acts as a hard Lewis acid and binds to hard donors such as oxygen. In its ionic form, zirconium exists as a both the ZrO^{2+} and Zr^{4+} ions.[10]

Table 1-2. Radionuclides of interest for PET imaging.[5,10]

Isotope	$t_{1/2}$	Energies (keV)
^{11}C	20.3 m	960
^{18}F	109.8 m	873
^{68}Ga	67.7 m	1899
^{86}Y	14.7 h	1221
^{64}Cu	12. 7 h	278
^{124}I	4.2 d	1532
^{89}Zr	78.4 h	396

Identification of free zirconium helps to determine the *in vivo* stability of a chelator. Zirconium has several different metabolic fates when freely introduced *in vivo*: bone, muscle tissue, and liver accumulation.[10] Where zirconium accumulates is dependent on the source used, the most common sources being zirconium oxalate, chloride, citrate, and phosphate. Accumulation in the bone of mice results from using zirconium oxalate, chloride, citrate, and phosphate. Zirconium citrate also accumulates in the muscle tissue and zirconium phosphate accumulates in the liver.[10] Identifying where each source of zirconium will accumulate will help identify if a complex is unstable.

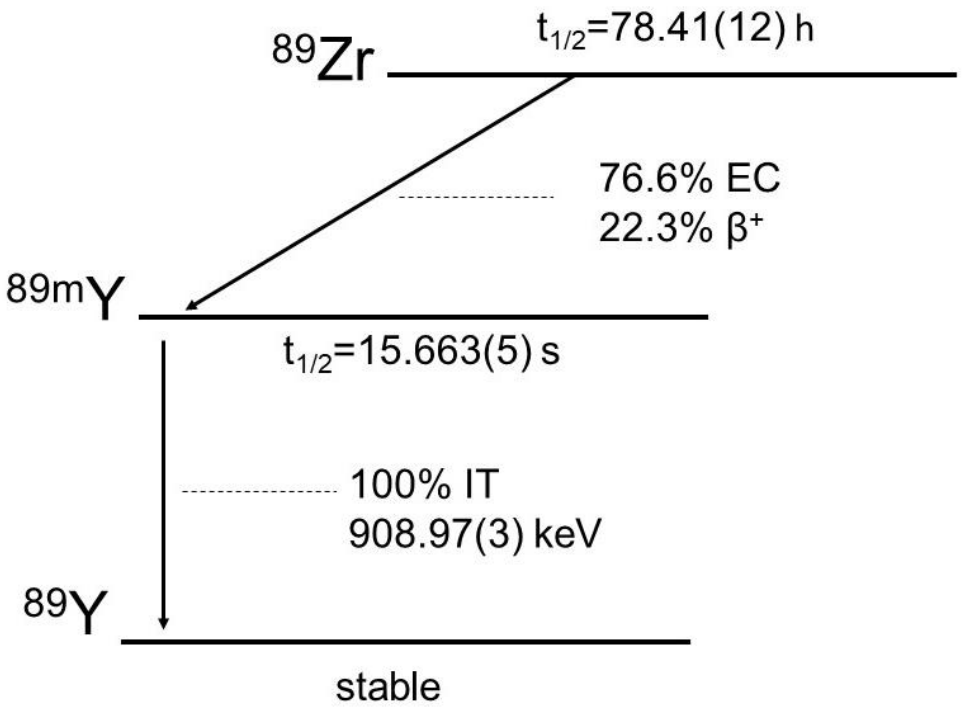

Figure 1-4. Decay pathway for zirconium-89.[8]

1.5 Chelators for Zirconium

1.5.1 Gold Standard for Zirconium

The current gold standard for ^{89}Zr chelation is the siderophore, desferrioxamine B, DFO **(5)** (Figure 1-5). DFO **(5)** is a commercially available compound under the trade name Desferal ©, which is clinically used in the neutralization of iron and aluminum overloads.[5,7] Clinical safety studies indicate that DFO **(5)** is not largely toxic and hence, no additional safety tests are required for other clinical trials. DFO **(5)** is the gold standard for $^{89}Zr^{4+}$ chelation because it is one of the few compounds in clinical use that forms a stable complex and has high *in vivo* stability.[5] The free primary amine functional group allows for many different coupling approaches to be used: thioester, succinyl, and thiocyanate groups.[11] The variety of linkers available for coupling has resulted in ^{89}Zr-DFO being tested with many different monoclonal antibodies, such as trastuzumab for breast cancer targeting.[11]

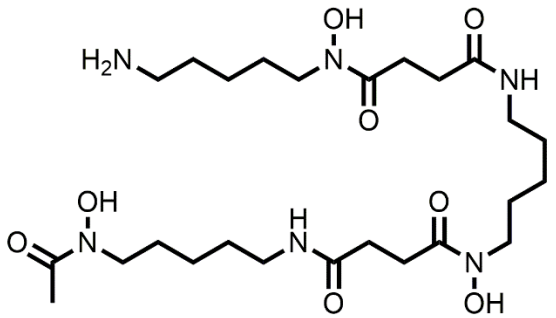

DFO, **5**

Figure 1-5. Gold standard for ^{89}Zr chelation, desferrioxamine B (DFO).

Though DFO **(5)** is the gold standard for ^{89}Zr chelation, there are some issues. The main concern is while the complex has high *in vivo* stability, there are cases where after 48 hours post injection free ^{89}Zr will begin to accumulate in the bone, suggesting decomplexation.[12] The lack of stability is proposed to be caused by DFO **(5)** forming a hexadentate complex where $^{89}Zr^{4+}$ prefers to be octa-coordinated, allowing two water molecules to coordinate.

1.5.2 Desferrioxamine-star

DFO **(5)** is the gold standard due to its clinical use for iron and aluminum overloads. While it is an attractive chelator for ^{89}Zr because it is safe to use, and approved, preclinical trials have shown uptake of ^{89}Zr in the bones resulting in a serious safety concern.[13] This complexation issue led to the development of the octadentate derivative of DFO **(5)**, Desferroxamine-star **(6)** (DFO*) (Figure 1-6).[13,14]

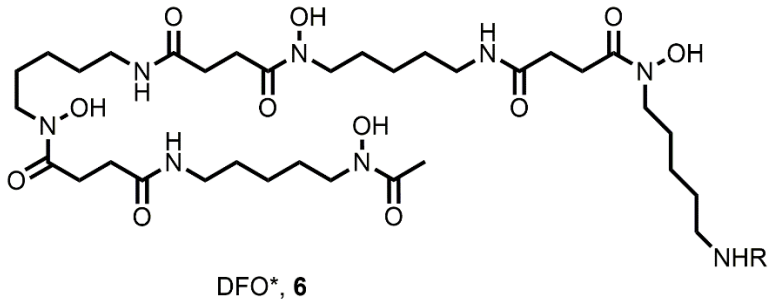

DFO*, **6**

Figure 1-6. Structure of the octadentate derivative of DFO.

DFO* **(6)** achieves a >95% radiochemical yield with ^{89}Zr after 5 minutes at room temperature at concentration 10^{-6} M.[14] Studies of bifunctional DFO* **(6)**, both *in vitro*

studies and *in vivo* have shown that ^{89}Zr-DFO*-trastuzumab is more stable than is ^{89}Zr-DFO-trastuzumab.[14] ^{89}Zr-DFO*-trastuzumab *in vitro* degrades slower than ^{89}Zr-DFO-trastuzumab at 4 °C over 72 hours at concentrations of 10^{-6} M, in human serum, and *in vivo,* has a lower uptake in the bones, liver, skin, and spleen than ^{89}Zr-DFO-trastuzumab.[14] Over time tumor uptake of the complex decreased with ^{89}Zr-DFO*-trastuzumab where as with ^{89}Zr-DFO-trastuzumab the uptake increased.[14] This indicated that the amount of free ^{89}Zr is greater with ^{89}Zr-DFO-trastuzumab over time.

While DFO* **(6)** appears to be a better chelator for ^{89}Zr than DFO **(5)** based on the stability of the complex, there is concern with the difficulty of the synthesis. DFO **(5)** and its derivatives are mostly insoluble making synthesis a challenge.[13] This insolubility affects both the synthesis of DFO* **(6)** and the bifunctional version of the ligand, which at most is synthesized in a 10% yield.[14]

1.5.3 Hydroxamate-based Ligands

Research for new chelators to replace DFO **(5)** has been increasing in the past few years. There are four main chelators that have been investigated for chelation of ^{89}Zr. Two of the ligands, based on the hydroxamate functional group, are Fusarinine C (FSC) **(7)** and H_4THL **(8)** (Figure 1-7).[15,16] FSC **(7)** is a hexadentate, macrocyclic chelating siderophore that is produced by fungi for iron acquisition from the environment and has been shown to be an excellent chelator for ^{68}Ga.[15] The appeal of FSC **(7)** as a chelator for Ga^{3+} is the ionic radius is similar in size to the ionic radius of Fe^{3+}.[15,17] For chelation with Zr^{4+}, the appeal is the hydroxamate functional groups similar to these in DFO **(5).** FSC **(7)** achieves a radiochemical yield of >95% at room temperature after 60 minutes at a concentration of 10^{-5} M.[15] The concern with FSC **(7)** is that the complexation is slower

than DFO **(5)**, due to macrocyclic chelators binding more slowly than non-macrocyclic chelators.[5] Current studies have only investigated FSC **(7)** chelating to ^{89}Zr for 24 hours at RT.[15]

H_4THL **(8)** is an non-macrocyclic, octadentate ligand designed as a zirconium chelator; however, due to the steric strain within the backbone the coordination of all arms to the metal is prevented, resulting in poor stability.[16] When compared to ^{89}Zr-DFO, both the methylene and ethylene forms of H_4THL **(8)** as a Zr^{4+} complex undergo decomplexation faster in mice plasma causing higher bone uptake for *in vivo* studies.[16] Reducing the steric constraints of the ligand is expected to improve its chelation to $^{89}Zr^{4+}$.

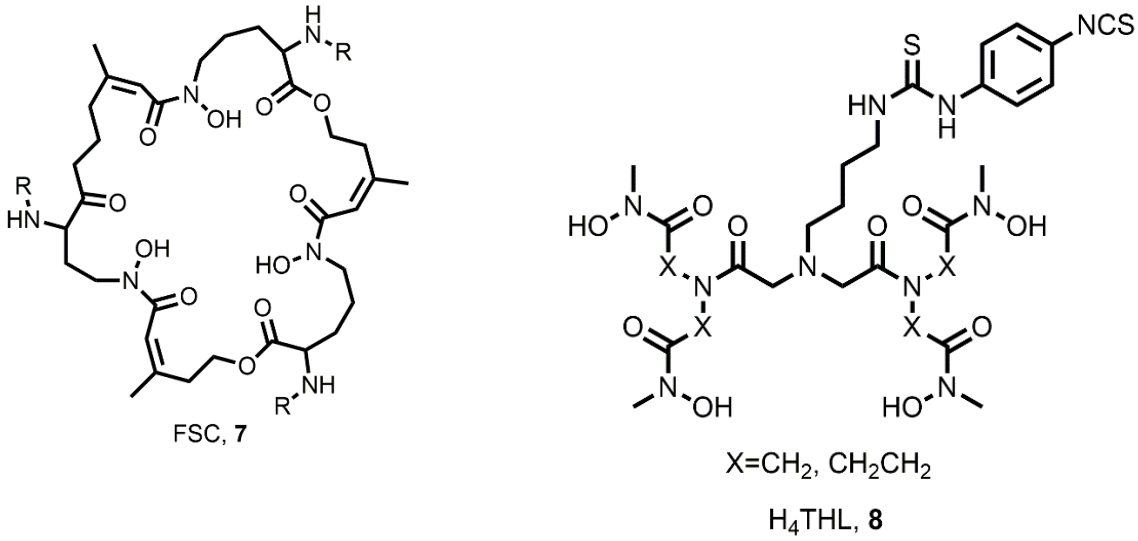

Figure 1-7: Hydroxamate-based ligands for zirconium chelation: Fusarinine C (FSC) and a tetrahydroxamate ligand (H_4THL).

1.5.4 Hydroxypyridinonate-Based Ligands

Two other ligands researched as a replacement for DFO **(5)** are the octadentate, non-macrocyclic, hydroxypyridinonate-based ligands, HOPO **(9)** and THPN **(10)** (Figure

1-8).[18–20] HOPO **(9)** has been shown to radiolabel easily with ^{89}Zr achieving 90% radiochemical yield in 1 h at room temperature, and the $^{89}Zr^{4+}$ complex is stable over a seven-day period at 37 ˚C in human serum.[18,19] ^{89}Zr-HOPO is overall more stable; however, the tumor uptake is around half of that of ^{89}Zr-DFO making DFO **(5)** a better ligand for PET.[18]

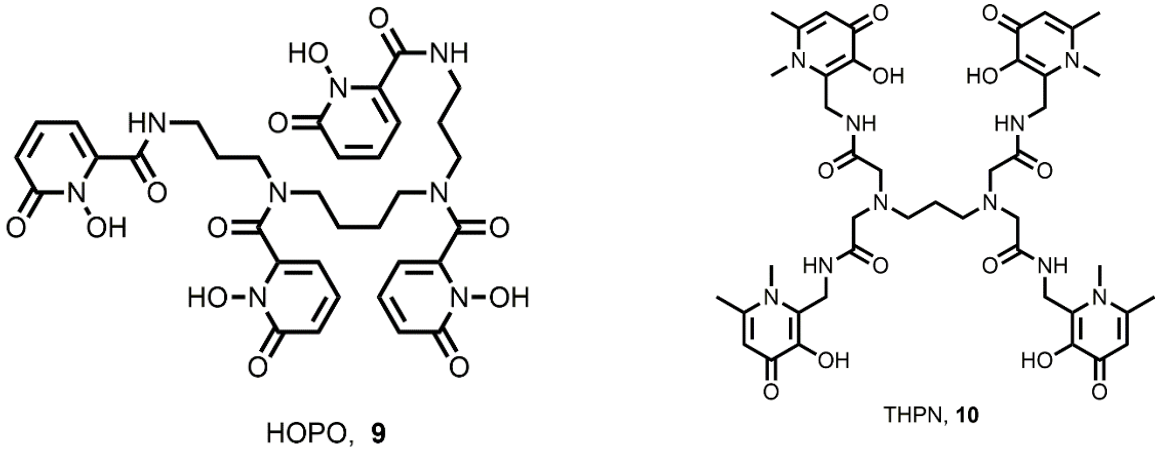

Figure 1-8. Hydroxypyridinonate-based ligands for zirconium chelation: THPN and HOPO.

The second hydroxypyridinonate-based ligand, THPN **(10)**, can achieve a radiochemical yield of >95% after 30 min at room temperature, at a concentration of 10^{-6} M, while DFO **(5)** labeling requires twice the time for similar results.[20] The bone uptake for ^{89}Zr-THPN is comparable to ^{89}Zr-DFO for *in vivo* showing that the complex is stable. While THPN **(10)** shows promise, a bifunctional form of the chelator has not been synthesized so tumor uptake cannot be examined. Even with new chelators being developed for ^{89}Zr, DFO **(5)** remains the gold standard.

1.6 Thesis Aims

The limitations of existing zirconium chelators for targeted imaging with ^{89}Zr shows a need for new ligands. This project began in our group with Dr. Sarah Spreckelmeyer, who synthesized the ligand H_4EDT(M)HA **(11)** to provide four hydroxamates to bind to the zirconium, which prefers to form octadentate complexes in an aqueous environment. It was found that H_4EDT(M)HA **(11)** has flexibility constraints preventing all four hydroxamates from binding to the zirconium, forming a 2:2 complex with ^{89}Zr .[21]

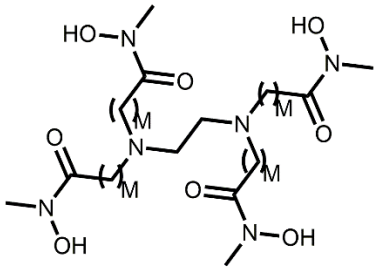

H_4EDT(M)HA, **11**
M= 1, 2

Figure 1-9. Structure of previous hydroxamate-based ligand H_4EDT(M)HA.[21]

To overcome the limitations of H_4EDT(M)HA **(11)**, a more flexible octadentate hydroxamate-based ligand is required. From these limitations, the ligands H_4octaha **(1)**, H_5decaha **(2)** and H_4noonha **(3)** were designed. H_4octaha **(1)** is an octadentate hydroxamate-based ligand that incorporates diethylenetriamine (dien) as a backbone. Like H_4octaha **(1)**, H_5decaha **(2)** incorporates dien as a backbone; however, the ligand incorporates an additional hydroxamate arm, generating a potentially decadentate chelator. H_4noonha **(3)** is an octadentate hydroxamate-based ligand that incorporates 1**,**2 bis(2-aminoethoxyl ethane) as a backbone. The functionalization of dien was also

pursued in order to synthesize bifunctional H_4octaha **(1)** and H_5decaha **(2)**. Herein, novel synthetic routes were developed for the synthesis of each of the three ligands and the functionalization of dien **(4)**.

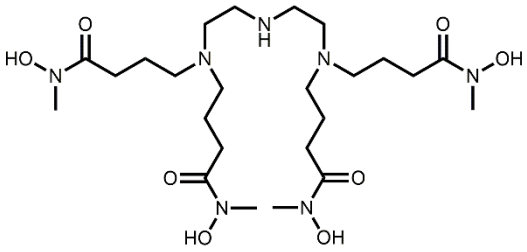

H_4octaha, **1**

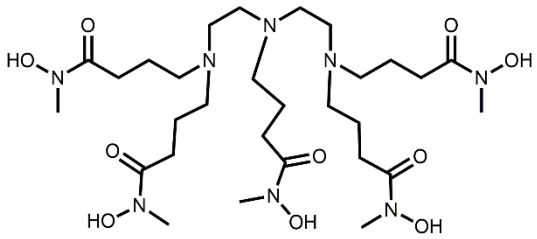

H_5decaha, **2**

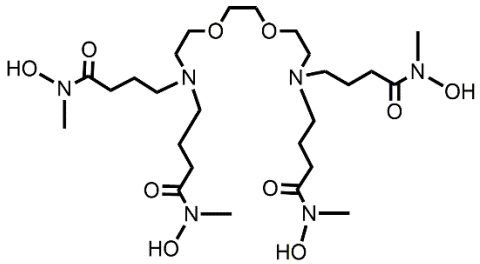

H_4noonha, **3**

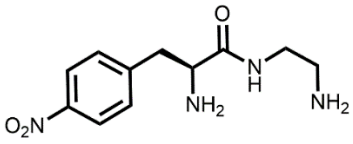

Functionalized dien, **4**

Figure 1-10. Novel hydroxamate-based, non-macrocyclic ligands for zirconium-89 chelation, and the bifunctional dien backbone.

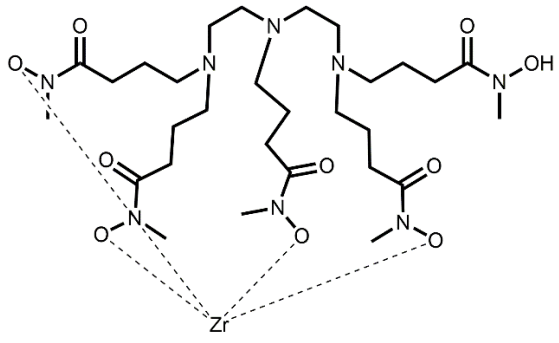

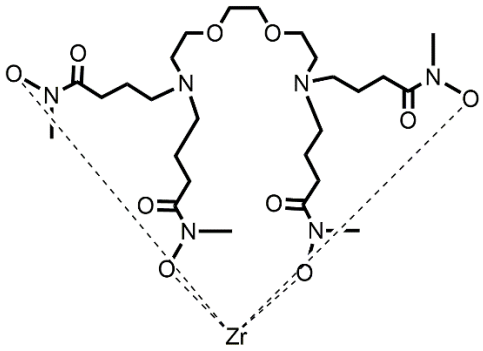

Figure 1-11. Proposed complexes for [Zr(decaha)] and [Zr(noonha)].

Chapter 2. Experimental

2.1 General

All solvents and reagents were purchased from commercial suppliers (Sigma Aldrich, Fischer Chemical, AK Scientific, Anachemia/VWR). ^{1}H NMR spectra were recorded at RT on a Bruker AV400 instrument on a Bruker Avance 300 spectrometer. Electrospray-ionization mass spectrometry (ESI-MS) was performed on a Waters LC-MS system consisting of an ESCI ion source and a Waters 2695 HPLC to deliver the samples. High-performance liquid chromatography (HPLC) was performed on a Waters HPLC system containing a Waters 66 controller, Waters 2487 dual wavelength absorbance detector, and a Waters delta 600 pump. A Phenomenex synergi 4u Hydro-RP 80A PX column (250 x 20 mm, 4 micron) was used for HPLC purification. Column chromatography was performed on a Teledyne Combiflash R_f automated column system. Centrifuging was performed on a VWR Clinical 50 centrifuge with 15 mL Falcon conical tubes. Solvent removal under vacuum was performed on a Heidolph Collegiate rotary evaporator with a BUCHI V700 vacuum pump.

2.2 Compounds for Synthesis of H_4octaha **(1)** (*Scheme 3-1*, Page 29)

2.2.1 Tert-butyl-hydroxy(methyl)carbamate[22] (12)

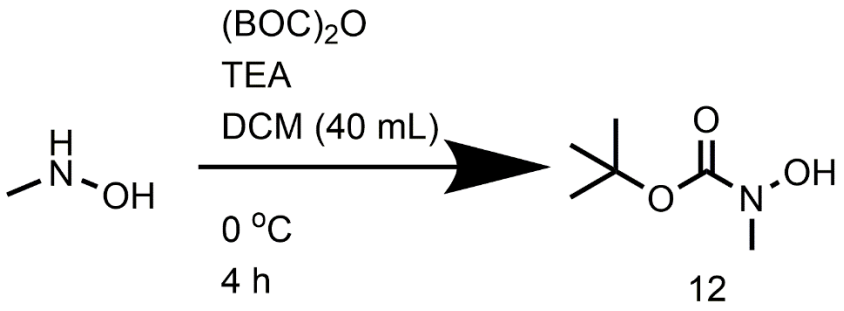

12

N-methylhydroxylamine hydrochloride (0.53 g, 6.3 mmol) was added to DCM (40 mL) at RT in a 50 mL round bottom flask. TEA (1 mL, 7.2 mmol) was added to the solution dropwise using a pipette and the resulting mixture was stirred for 20 min until complete dissolution. Boc_2O (1.53 g, 7.0 mmol) was added and the solution was stirred for 4 h at 0 °C. The solution was then removed from the ice bath and an air stream was used to remove the solvent for 1 h, resulting in a colourless oil and white crystals. The crude product was used directly in the following reaction. ESI-MS: calcd. for $[C_6H_{13}NO_3+H]^+$: 148.1; found 148.3 $[M+H]^+$.

2.2.2 Tert-butyl-N-benzyloxy-N-methylcarbamate[23] (13)

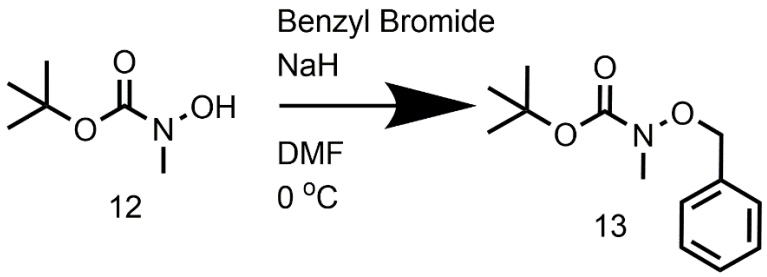

Crude compound **12** (1.96 g) was dissolved in acetone and transferred from a 50 mL round bottom flask to a 100 mL 2-neck round bottom flask with a septum. The mixture was put under vacuum for 1 h to remove the acetone. Dry DMF (30 mL) was added to the flask to dissolve the crystals at 0 °C. The system was flushed with argon gas, and sodium hydride 60% (0.605 g, 14.8 mmol) was slowly added to the solution and the reaction mixture stirred for 30 min at 0 °C. Benzyl bromide (1.70 mL, 14.3 mmol) was slowly added to the solution by syringe and stirred for 4 h. Hexanes (5 mL) was added to the solution to create an organic layer on top and the solution was quenched with ethyl acetate, methanol, and water to destroy any unreacted sodium hydride. The organic phase was separated, and hexanes removed under vacuum to create a mixture of yellow oil and solid. The product was purified by column chromatography on a 24 g silica column (A: hexanes, B: ethyl acetate, 100% A to 100% B gradient) to yield a yellow oil **13** (0.277 g, 9%). ^{1}H NMR (400 MHz, $CDCl_3$, RT): 1.51 (s, 9H), 3.06 (s, 3H), 4.84 (s, 2H), 7.28-7.41 (m, 5H). ESI-MS: calcd. for $[C_{13}H_{19}NO_3+Na]^+$: 260.1; found 260.1 $[M+Na]^+$.

2.2.3 O-Benzyl-N-methyl-hydroxylamine[24] (14)

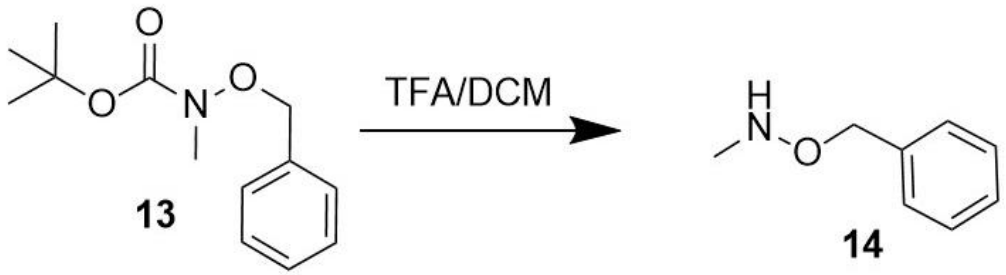

Compound **13** (0.277 g, 1.17 mmol) was dissolved in TFA/DCM (1:1) (2 mL) at RT in a 25 mL round bottom flask and the resulting solution was stirred overnight. The solvent was removed under vacuum and the resulting orange oil was purified by column chromatography on a 12 g HP silica column (A: hexanes, B: ethyl acetate, 100% A to 100% B gradient) to yield a light-yellow oil **14** (0.150 g, 93%). ^{1}H NMR (400 MHz, CD_3OD, RT): 2.93 (s, 3H), 5.05 (s, 2H), 7.38 (s, 5H). ESI-MS: calcd. for $[C_8H_{11}NO+H]^+$: 138.1; found 138.2 $[M+H]^+$.

2.2.4 O-Benzyl-4-bromo-N-methylbutahydroxamic acid[23] (15)

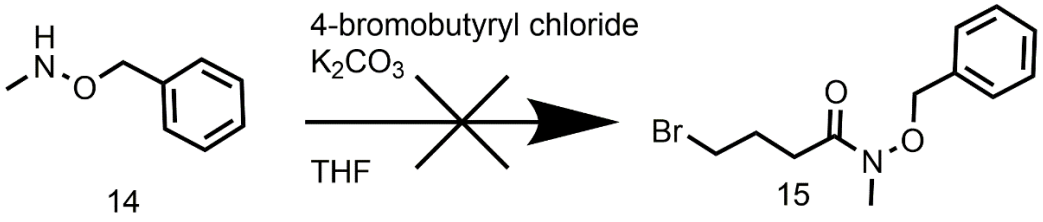

Compound **14** (0.152 g, 1.11 mmol) was added to a 25 mL round bottom flask with anhydrous potassium carbonate (0.269 g, 1.95 mmol) in dry THF (3 mL) and was stirred for 15 min at 0 °C. 4-Bromobutyryl chloride (0.150 mL, 1.30 mmol) was slowly added to the solution and the resulting mixture was stirred for 7 h at 0 °C. The solution was placed in a 15 mL conical tube and centrifuged. The liquid was decanted into a 25 mL round bottom flask to remove the anhydrous potassium carbonate and the solvent was removed under vacuum producing a yellow oil which was purified by column chromatography on a 12 g HP silica column (A: hexanes, B: ethyl acetate, 100% A to 100% B gradient). Satisfactory characterization data was never obtained.

2.3 Compounds for Synthesis of H_5decaha **(2)** (*Scheme 3-2*, Page 31)

2.3.1 Diethylenetriamine-penta(ethyl butyrate)[25] (16)

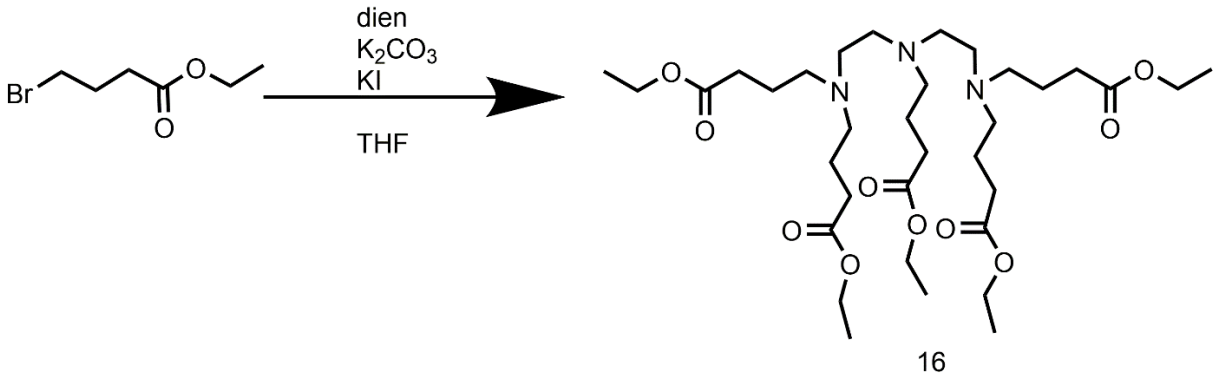

16

Diethylenetriamine (0.100 mL, 0.93 mmol) was added to a 50 mL round bottom flask with anhydrous potassium carbonate (0.821 g, 5.94 mmol) and potassium iodide (0.782 g, 4.70 mmol) in dry THF (5 mL) under argon. The mixture was stirred for 15 min and ethyl-4-bromobutyrate (0.700 mL, 4.89 mmol) was added to the solution. The solution was stirred for 48 hours and the solvent was removed under vacuum to produce a crude yellow oil which was purified by column chromatography on a 24 g HP silica column (A: ethyl acetate, B: methanol, 100% A to 5% B gradient) to yield a light-yellow oil **16** (0.1827 g, 6%). ^{1}H NMR (400 MHz, $CDCl_3$, RT): 1.22-1.29 (m, 18H), 1.77 (s, 9H), 2.32-2.35 (m, 11H), 2.49-2.51 (m, 13H), 4.11-4.16 (m, 10H). ESI-MS: calcd. for $[C_8H_{11}NO+H]^+$: 674.2; found 674.5 $[M+H]^+$.

2.3.2 H_5decaha (diethylenetriamine-penta(propylene-N-methylhydroxamic acid)[21] (2)

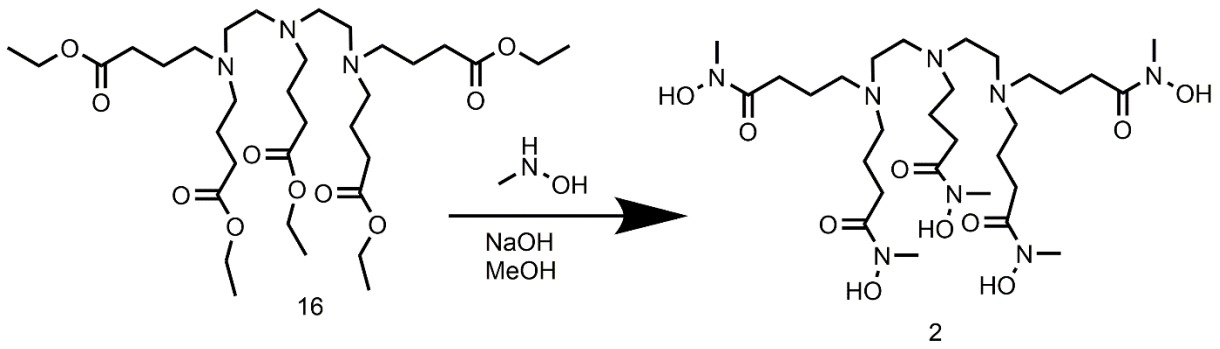

N-methylhydroxylamine hydrochloride (0.144 g, 1.72 mmol) and sodium hydroxide (67.2 mg, 1.68 mmol) were added to dry methanol (2 mL) in a 25 mL round bottom flask and stirred for 15 min until dissolved. Compound **16** was dissolved in dry methanol (1 mL) and was slowly added to the solution. The solution was stirred for 48 hours at RT and the solvent was removed under vacuum to produce a brown solid. The brown solid was dissolved in deionized water and acidified with 1 M HCl to pH 1. The solution was then purified by semi-prep reverse-phase HPLC (10 mL/min, gradient A: 0.1% TFA in deionized H_2O, B: acetonitrile, A: 95% to B: 100% for 25 min, t_R=11.32 min). Insufficient sample was obtained for NMR spectroscopy. ESI-MS calcd. for $[C_{29}H_{58}N_8O_{10}+K]^+$ 718.3; found 718.4 $[M+K]^+$.

2.4 Compounds for the Synthesis of H_4noonha **(3)** (*Scheme 3-3*, Page 35)

2.4.1 N,N,N,N-Tetra(ethyl-butyrate)-1,2 bis(2-aminoethyoxyl) ethane[25] (17)

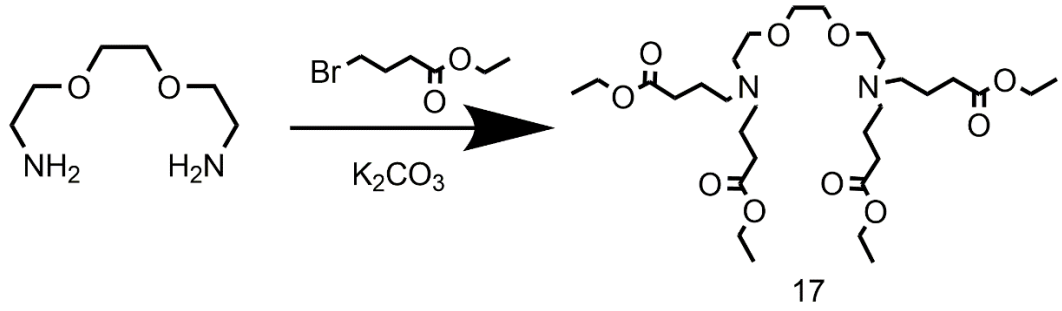

17

Potassium carbonate (4.205 g, 30.42 mmol) was added to a 50 mL round bottom flask in dry THF (8 mL). The mixture was stirred for 15 min and ethyl-4-bromobutyrate (4.3 mL, 29.45 mmol) and 1,2-bis(aminoethoxylethane) (0.5 mL, 3.41 mmol) were added to the solution and stirred for 48 hours and a salt formed. The salt was filtered out and the solvent was removed under vacuum to produce a crude yellow oil which was purified by column chromatography on a 24 g HP silica column (A: ethyl acetate, B: methanol, 100% A to 10% B gradient) to yield a light-yellow oil **17** (18%, 374 mg). ^{1}H NMR (400 MHz, $CDCl_3$, RT): 1.23-1.26 (m, 12H), 1.69-1.77 (m, 10H), 2.28-2.32 (t, J= 4 Hz, 8H), 2.46-2.49 (t, J= 8 Hz, 8H), 2.61-2.65 (t, J= 8 Hz, 4H), 3.48-3.66 (m, 8H), 4.09-4.14 (m, 8H). ESI-MS: calcd. for $[C_{30}H_{56}N_2O_{10}+H]^+$: 605.1; found 605.5 [M+H]. for $[C_{30}H_{56}N_2O_{10}+K]^+$: 643.3; found 643.1 $[M+K]^+$.

2.4.2 H_4noonha (N,N,N,N-Tetra-(N-methylbutohydroxamic acid)-1,2 bis(2-aminoethoxyl ethane)[26] (3)

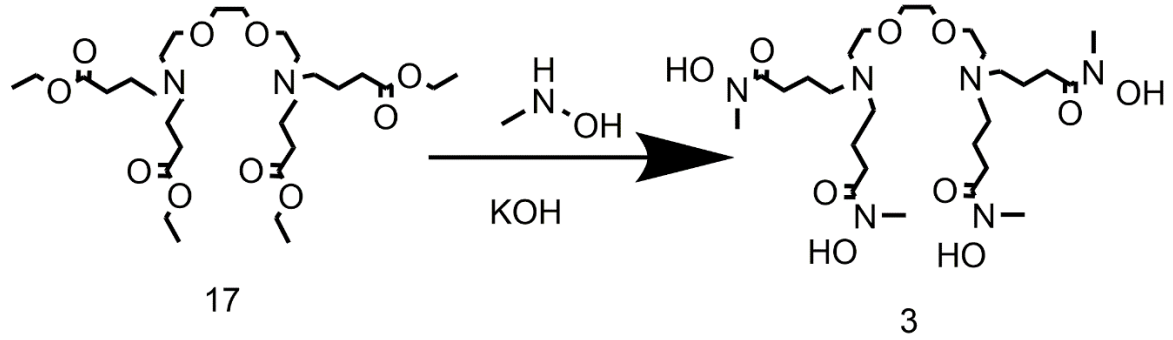

17 3

Compound **17** (0.163 g, 0.270 mmol) was added to methanol (3 mL) in a 50 mL round bottom flask. The mixture was stirred for 10 minutes and N-methylhydroxylamine hydrochloride (0.228 g, 2.73 mmol) was added to the solution. Potassium hydroxide (0.229 g, 4.08 mmol) was dissolved in 1 mL of deionized water and this solution was added dropwise to the 50 mL round bottom flask. The mixture was stirred for 48 hours forming a salt. The salt was filtered out of solution and the solvent was removed under vacuum to produce a crude yellow oil which was dissolved in deionized water and acidified with 1 M HCl to pH 1. The solution was then purified by semi-prep reverse-phase HPLC (10 mL/min, gradient A: 0.1% TFA in deionized water, B: acetonitrile, A: 100% to B: 40% for 42 min., t_R=13.48 min). The purified product was purified further by semi-prep reverse-phase HPLC (10 mL/min, gradient A: 0.1% TFA in deionized water, B: acetonitrile, A: 100% to B: 25% for 52 min., t_R=32.57 min) to produce a yellow solid **(3)** (18%, 30 mg). ^{1}H NMR (300 MHz, D_2O, RT): 2.90-2.94 (t, J=6 Hz, 4H), 3.09-3.21 (m, 24H), 3.29-3.34 (m, 8H), 3.46-3.50 (t, J=6 Hz, 4H), 3.65-3.74 (m, 16H). ESI-MS: calcd. for $[C_8H_{11}NO+H]^+$: 608.4; found 608.1 $[M+H]^+$.

2.5 Compounds for synthesis of functional dien (*Scheme 3-4*, Page 37)

2.5.1 N-(2-Aminoethyl)-p-nitrophenylalanine amide[27] (4)

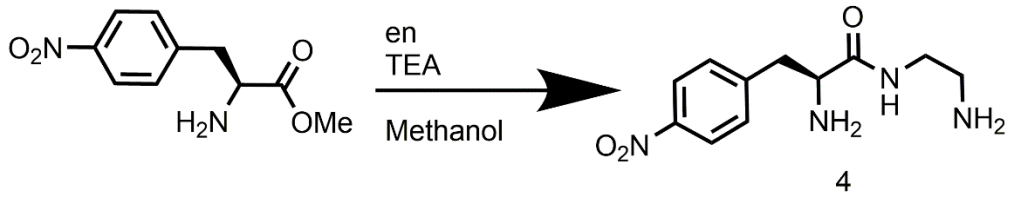

4

Nitro-L-phenylalanine methyl ester HCl (0.505g, 1.94 mmol) was mixed with TEA (0.300 mL, 2.20 mmol) in methanol (2 mL) and stirred for 15 min at RT. The solution was then added dropwise to en (3.70 mL, 55.4 mmol) resulting in a bright green solution. The solution was stirred overnight at RT until the solution turned dark red. Concentrated hydrochloric acid (2 mL) was added to the solution and the product was precipitated out as a HCl salt **(4)**. ^{1}H NMR (400 MHz, CD_3OD, RT): 2.73 (s, 2H), 2.98 (s, 2H), 3.27 (s, 2H), 3.60 (s, 1H), 7.49 (s, 2H), 8.20 (s, 2H). ESI-MS: calcd. for $[C_{11}H_{16}N_4O_3+H]^+$: 253.253; found 253.3 $[M+H]^+$.

Chapter 3. Results and Discussion

3.1 Synthesis of octadentate hydroxamate ligand, H_4octaha **(1)**

The approach to H_4octaha **(1)** was based on the work of a former PhD student in the Orvig group, Dr. Sarah Spreckelmeyer. The original ligand idea, H_4EDT(M)HA **(11)**, had limitations with flexibility in the backbone and the arms, preventing all arms binding to $^{89}Zr^{4+}$. Ligand complexation involved two ligands binding to two Zr^{4+} ions creating a 2:2 metal:ligand complex, which also was observed with H_4THL **(8)**.[16] To solve this issue the backbone was extended from en to dien and the carbon chains on the arms were extended from ethyl to butyl, to suggest **1** (*Scheme 3-1*).

The secondary amine of N-methylhydroxylamine was first boc protected using Boc_2O to produce compound **12** (*Scheme 3-1*). The synthesis has difficulties with the purification; owing to this, compound **12** was used without further purification in the subsequent step.[21] The hydroxamic acid was protected using a benzyl group to produce a yellow oil **(13)**. The ^{1}H NMR spectrum, Figure A-1, shows a 9H singlet at 1.51 ppm indicating the boc protection, a 5H multiplet at 7.38 ppm and a 2H singlet at 4.84 ppm indicating the benzyl protection, and a 3H singlet at 3.06 ppm corresponding to the methyl group. The boc protecting group was then removed from compound **13** to generate compound **14** in a yield of 93%. The ^{1}H NMR spectrum, Figure A-2, shows the disappearance of the characteristic 9H singlet peak corresponding to the boc-group confirming the deprotection. The synthesis for compound **15** was attempted but was unsuccessful.

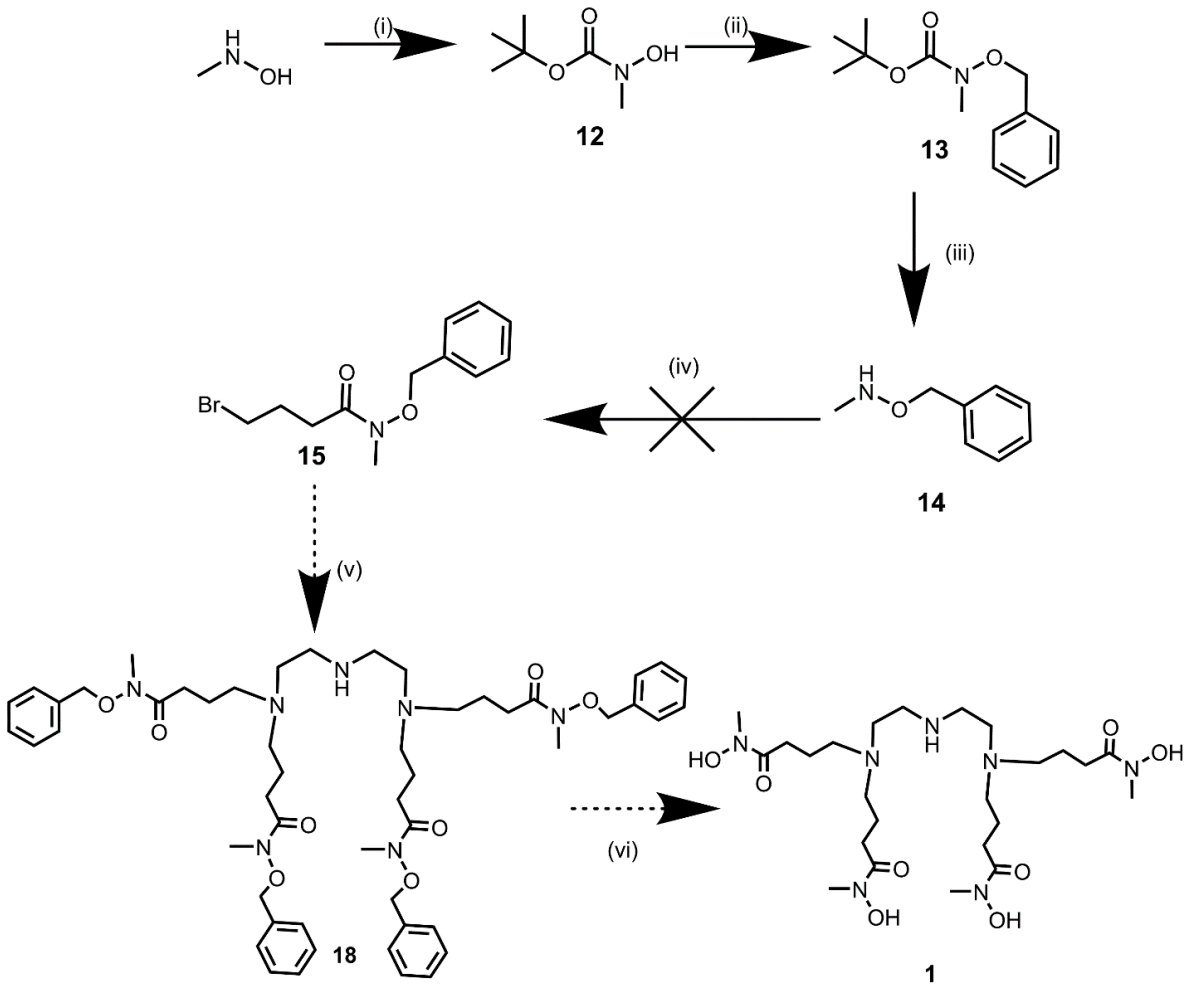

Scheme 3-1. Synthesis of H_4octaha: Reagents and conditions: i) Boc_2O, CH_2Cl_2, 0 °C; ii) NaOH, $C_6H_5CH_2Br$, 0 °C; iii) TFA/CH_2Cl_2, RT; iv) K_2CO_3, $Br(CH_2)_3COCl$, THF, RT; v) dien, K_2CO_3, ACN, 0 °C; vi) $Pd(OH)_2$/C, H_2, MeOH, RT.

A possible issue with the synthesis of compound **15** might be that 4-bromobutyryl chloride is cyclizing with the before it reacts with 4-bromobutyric acid before it can react with compound **14**. This side reaction also explains the reported low yield for the similar step in the synthesis of H_4EDT(M)HA **(11)**.[21] Another issue with the synthesis of H_4octaha **(1)** was the lack of control in the amine alkylation of secondary amines after the addition of two arms for compound **(18)**. The structure of H_4octaha **(1)** has the central nitrogen of

the dien backbone as a 2˚ nitrogen. The central nitrogen is more likely to be alkylated than the other nitrogen atoms in the dien backbone, after the addition of two arms. This results in a mixture of four arms alkylating different secondary amines creating a mixture of different octadentate hydroxamate ligands, making purification difficult. The control and purification issue can be solved with a different synthetic route.

3.2 Synthesis of decadentate hydroxamate ligand, H_5decaha **(2)**

The synthesis of H_5decaha **(2)** was designed to overcome the issues arising during the synthesis of H_4octaha **(1)**. The first issue was with the synthesis of the hydroxamate arm **(15)**, in a very low yield, with a side product. The second issue was the lack of control when alkylating the amines of the dien backbone. *Scheme 3-1* was discussed with, Dr. Xiaozhu Wang, a postdoctoral fellow in the group, to develop a method to avoid the issues previously discussed. *Scheme 3-2* was developed to synthesize the decadentate ligand, H_5decaha **(2)**. The original project proposal was to produce an octadentate hydroxamate-based ligand to bind $^{89}Zr^{4+}$. While H_5decaha **(2)** exceeds this expectation, as a potentially decadentate ligand it will still be useful for complexation with other radiometal ions such as Ac^{3+}.

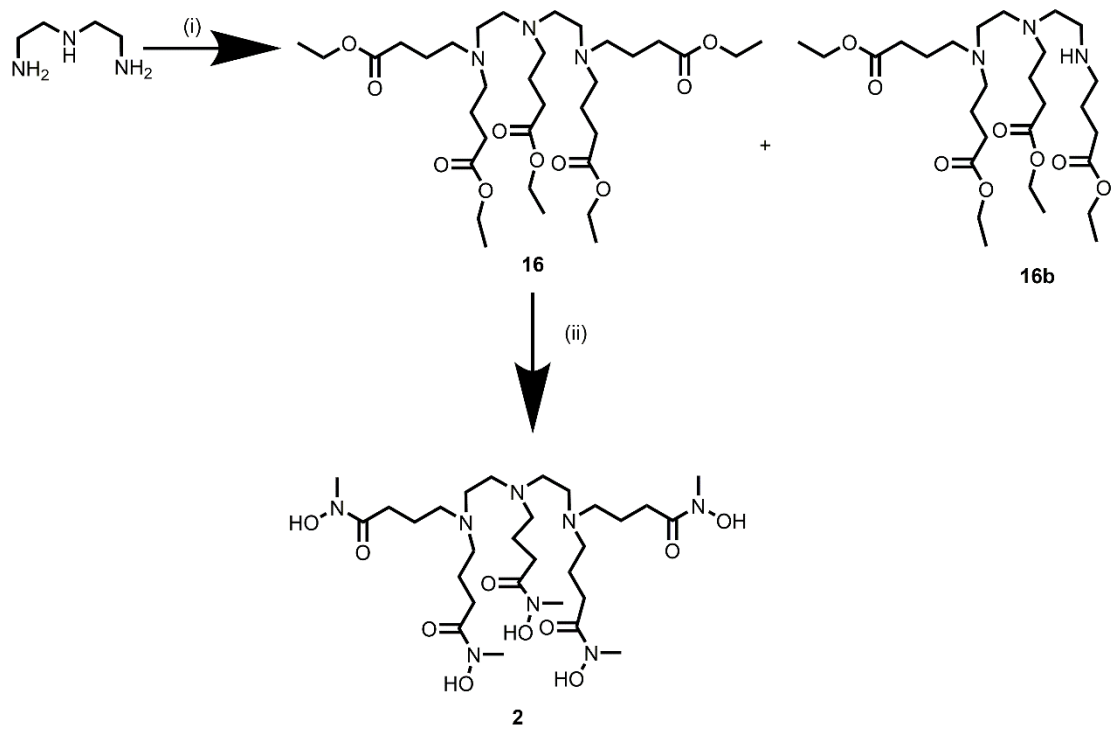

Scheme 3-2. Synthesis of H_5decaha. Reagents and conditions: i) $Br(CH_2)_3COOC_2H_5$, K_2CO_3, KI, THF, RT; ii) CH_3NHOH, NaOH, dry MeOH, RT.

Ethyl-4-bromobutyrate was converted to the corresponding iodide via a Finkelstein reaction using KI with dry acetone.[24] Diethylenetriamine was then reacted via S_N2 with 5 equivalents of ethyl-4-iodobutyrate to alkylate the amines present in the dien backbone to generate compound **16**. The product was then purified by column chromatography; however, the yield for compound **16** is difficult to determine without further purification. In the ESI-MS spectrum, peaks for m/z= 560 and 674 were present, which correspond to the side product **(16b)** and compound **16,** respectively. The ^{1}H NMR spectrum, Figure A-3, shows several signals that indicate that the product was not pure. The 10H multiplet from 4.11 ppm to 4.16 ppm corresponds to the five -CH_2- groups in the ester protection group. The 11H multiplet peak from 2.32 ppm to 2.35 ppm and the 13 H multiplet peak

from 2.49 to 2.51 ppm correspond to 14 -CH_2- groups the have similar chemical environments; the four -CH_2-groups in the dien backbone, two -CH_2- groups in each arm. The two -CH_2- groups in each arm are the -CH_2- groups in the propyl arm connected to the dien backbone and the -CH_2- groups in the propyl arm that connects the ethyl ester. The total integration of these multiplets should be 28H but is ~24H which is possible causes by the mixture of **16** and **16b**. The peak at 1.77 ppm should correspond to the central CH_2-group in the propyl arm; however, the integration is < 10. The multiplet peak from 1.22 ppm to 1.29 ppm should correspond to the five -CH_3 of the ethyl protection group in each arm; however, the integration was > 15. The differences in the integration of the peaks indicate a mixture of compounds **16** and **16b,** which would have similar spectra. While it is possible to purify the product further by HPLC, it was decided to continue with the synthesis and purify after H_5decaha **(2)** had been synthesized.

The semi-pure compound **16** was reacted with 10 equivalents of N-methylhydroxylamine and 12 equivalents of potassium hydroxide to convert the ethyl ester groups into hydroxamates. Following stirring for 48 hours, H_5decaha **(2)** is purified by semi-prep HPLC. After purification by semi-prep HPLC there was not enough sample obtained to perform analysis by NMR. The low-resolution mass spectrum contained a peak at 701.4 which may correspond to the $[M+K]^+$ ion of H_5decaha **(2)**.

The low-resolution mass spectrum suggests that H_5decaha **(2)** was formed; however, without ^{1}H NMR and ^{13}C NMR spectra, the formation of H_5decaha **(2)** cannot be confirmed. With the limited amount of purified H_5decaha **(2)** an addition test involving Ga^{3+} complexation was used to further support the synthesis. Ga^{3+} has two stable isotopes, ^{69}Ga and ^{71}Ga, with an isotope ratio of 60:40. When complexed with H_5decaha

(2) two unique peaks should appear within the mass spectra. Gallium nitrate was added to H_5decaha **(2)** in methanol and stirred for 10 minutes. The solution was then analysed by low-resolution mass spectrometry. The spectrum contained peaks at m/z=789.1 and 791.1 that correspond to $[^{69}Ga(Na_2decaha)+H]^+$ and to $[^{71}Ga(Na_2decaha)+H]^+$ respectively. These results are promising for the synthesis of H_5decaha **(2);** however, the purification method needs to be optimized to obtain enough purified H_5decaha **(2)** for ^1H NMR and ^{13}C NMR analysis.

3.3 Synthesis of octadentate hydroxamate ligand, H_4noonha

H_4noonha **(3)**, an octadentate chelator, was developed to help overcome the difficulty of synthesis with the dien backbone in H_4octaha **(1)** and H_5decaha **(2)**. *Scheme 3-3* was developed using a modified version of the synthetic methodology for H_5decaha **(2)** with the substitution of the dien backbone with 1,2-bis(aminoethoxylethane). Using the 1,2-bis(aminoethoxylethane) backbone allows for only 4 ethyl ester arms to be attached consistently and reduces the formation of side products. The denticity of H_4noonha **(3)** combined with the flexibility of the arm should make the ligand an excellent chelator for $^{89}Zr^{4+}$.

1,2-Bis(aminoethoxylethane) was reacted with 4.4 equivalents of ethyl-4 bromobutyrate via S_N2 to generate compound **17**. Compound **17** was purified by column chromatography; however, because compound **17** is not UV active, compound **17** was detected by TLC using potassium permanganate stain. In the ESI-MS spectrum, the peaks for 604 and 643 correspond to **17**+$[H^+]$ and **17**+$[K^+]$ respectively. The ^1H NMR spectrum, Figure A-4, shows several peaks that indicate that compound **17** is not

completely pure. The 12H multiplet from 1.23 ppm to 1.27 ppm corresponds to the -CH_3 group of the ethyl protection group for each arm. The 8H multiplet from 1.69 ppm to 1.77 ppm corresponds to the -CH_2- in the middle of each arm. The triplets from 2.29 ppm to 2.32 and from 2.46 ppm to 2.49 ppm represent the remaining -CH_2- hydrogen atoms within the arm. The triplet from 2.60 ppm to 2.65 ppm integrating to ~4 hydrogen atoms corresponds to the -CH_2- group within the backbone, closest to the N-atom. The triplet from 3.49 ppm and 3.52 ppm with an integration of ~4H and the multiplet from 3.56 ppm to 3.65 ppm correspond to the remaining 8H -CH_2- in the backbone; however, it is too difficult with just the ^{1}H NMR results to determine which set of peaks correspond to which -CH_2- as the chemical environments are very similar. The multiplet from 4.08 ppm to 4.14 ppm corresponds to the -CH_2- group in the ethyl protection group. Compound **17** was determined to be pure enough to continue with the synthesis of H_4noonha **(3)**.

Compound **17** was then reacted with N-methylhydroxylamine hydrochloride in a 10:1 excess per ester for a total excess of 40:1 of N-methylhydroxylamine hydrochloride to compound **17**. The addition of potassium hydroxide in water to the previous solution caused the solution to go cloudy. After stirring for 48 hours, the solvent was removed by vacuum under pressure, and the crude product was purified on semi-prep HPLC. The first purification consisted of a mixture of H_4noonha **(3)** and a side product where one of the ethyl esters was not converted into a hydroxamate. The semi-pure H_4noonha **(3)** mixture was further purified by semi-prep HPLC to separate H_4noonha from the side product resulting in a yield of 18%. Optimizing the purification method so that purification only requires one run on HPLC rather than two will increase the yield. The time constraints of this project prevented this optimization.

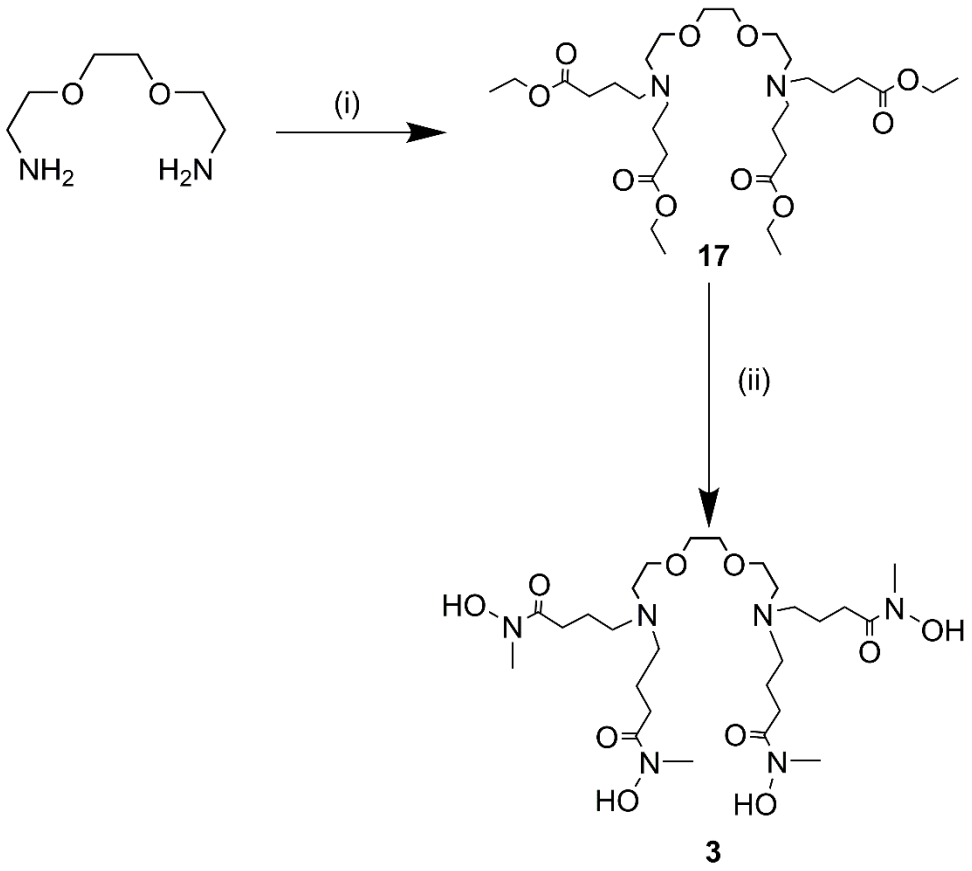

Scheme 3-3. Synthesis of H_4noonha. Reagents and conditions: i) $Br(CH_2)_3COOC_2H_5$, K_2CO_3, THF, RT; ii) CH_3NHOH, KOH in H_2O, MeOH, RT.

The ^{1}H NMR spectrum, Figure 3-1, shows several peaks that support the synthesis and purification of H_4noonha **(3)** as well as some peaks that indicate that there is a contamination. The 4H multiplet from 2.90 ppm to 2.94 ppm corresponds to the two -CH_2- groups in the backbone closest to the nitrogen atoms. The 24H multiplet from 3.09 ppm to 3.21 ppm corresponds to the -CH_3 groups and the central -CH_2- groups of the backbone. The doublet of doublets from 3.29 ppm to 3.4 ppm integrating to 8 H corresponds to the -CH_2- in the middle of the arm. The triplet from 3.46 ppm to 3.50 ppm with an integration of 4H corresponds to the remaining two -CH_2- groups in the backbone. The remaining 16H multiplet from 3.65 ppm to 3.74 ppm represents the remaining eight -

CH_2- in the arms (Figure 3-1). The other peaks in the ^1H NMR spectrum indicate that the sample became contaminated. The multiplet from 1.30 ppm to 1.33 ppm possibly corresponds to solvent. The multiplet from 7.43 ppm to 7.53 ppm and from 8.15 ppm to 8.23 ppm within the aromatic region corresponds to an unknown contaminant. Additional purification and optimization of the synthesis was attempted; however, due to time constraints of the project neither of these were fully successful. Once the optimization of synthesis has been completed and enough purified H_4noonha **(3)** has been obtained then the remaining analyses on the ligand can be performed.

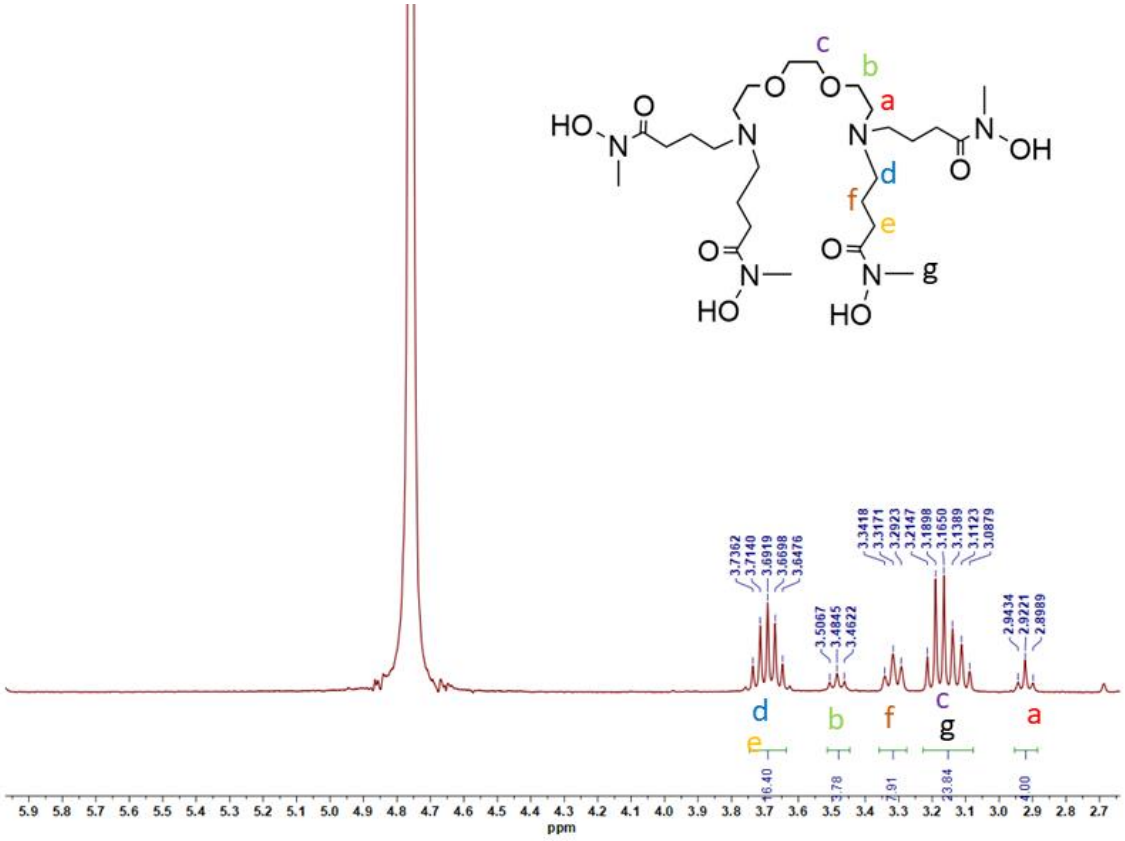

Figure 3-1. ^1H NMR spectrum of H_4noonha **(3)** peaks of interest (300 MHz, D_2O, 298 K).

3.4 Synthesis of functionalized diethylenetriamine backbone

For a ligand to become a BFC, a functional group for attaching a linker is required. While there are many ways to do this, many of the BFCs in the Orvig group functionalize through the backbone rather than through an arm. The approach to a functionalized dien is like the functionalization of chelators that use an en backbone and functionalized through a carbon atom. There are two forms of the functionalized backbone that can be used for creating a BFC (*Scheme 3-4*). The functionalized diethylenetriamine backbone **(4)** consists of an amide group that prevents the alkylation of the central amine allowing for only four arms to be attached creating a possible octadentate ligand. The second form of the backbone that can be used is the reduced form of the functionalized dien backbone, compound **19**. Compound **19** has the amide reduced to a secondary amine allowing for five arms to be attached.

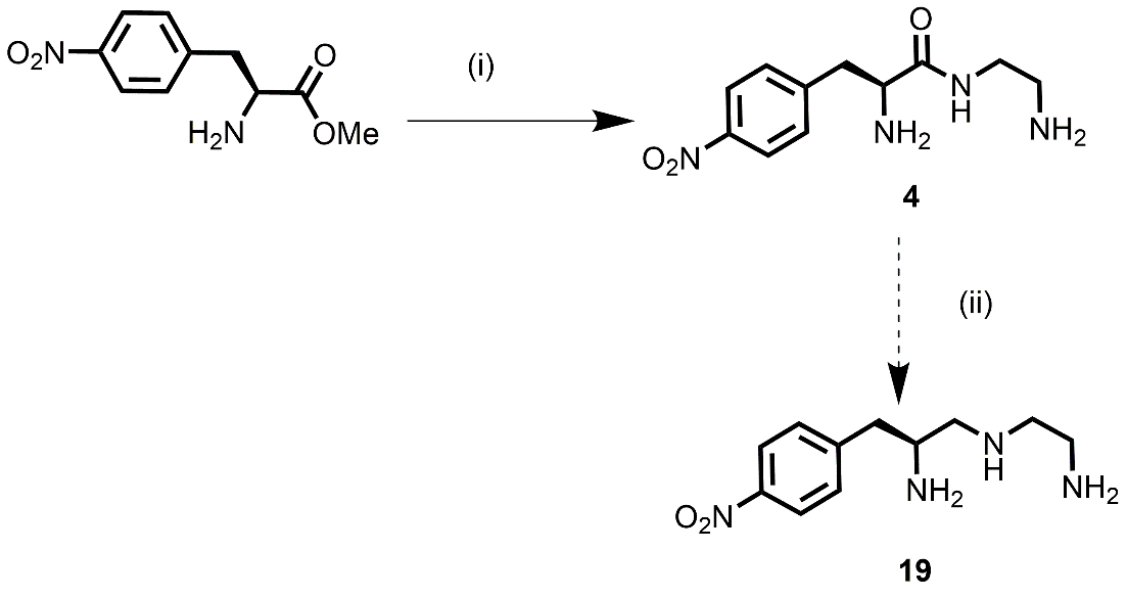

Scheme 3-4. Synthesis of functionalized diethylenetriamine. Reagents and conditions: i) en, TEA, MeOH, RT; ii) BH_3·THF, MeOH, Ar, ~50 °C.

The ^{1}H NMR spectrum, Figure 3-2, indicates that compound **4** was synthesized; however, there are several issues with obtaining a pure sample. The 2H singlet at 2.73 ppm corresponding to the -CH_2- group farthest from the functionalization point in the backbone. The 2H singlet peak at 2.98 ppm corresponds to the next -CH_2- group. The 2H singlet peak at 3.27 ppm corresponds to the -CH_2- group in the functional group. The 1H singlet peak at 3.60 ppm corresponds to the only -CH- group in compound **4** at the functionalization point in the dien. The remaining peaks at 7.49 ppm and 8.20 ppm correspond to the four hydrogen atoms within the aromatic ring of the para-nitro benzyl group. There are two peaks at 2.86 ppm and 3.33 ppm, most likely from the initial reactants.

The challenge with this reaction is with purifying the final product from the reactants. The original method for purifying involved removing the solvent and reactants at 50 °C under vacuum for 24 hours.[27] The issue with this method was that even after 48 hours under vacuum pressure the reagents were not fully removed. To try and further purify compound **4,** the semi-purified mixture was further purified by column chromatography; compound **4** sticks to the column causing it to streak making purification difficult. The other method that was attempted to purify compound **4** was to precipitate it out as an HCl salt; this method was used for achieving the sample used for ^{1}H NMR analysis. The difficulty with the HCl salt is the insolubility of the compound, making analysis and future synthesis more difficult.

The bifunctional dien backbone **(4)** requires further purification and analysis before use. After the backbone has been fully purified and characterized, the bifunctional forms of H_4octaha **(20)** and H_5decaha **(21)** (*Scheme 3-5*) can be synthesized using the same

methodology as for H_5decaha **(2)**. A difficulty with the synthesis of H_4octaha **(1)** is the lack of control in the alkylation of the amines in the dien backbone; this was solved with the synthesis of H_5decaha **(2)**, where all amines reacted with the ligand arms solving the selectivity issue. With the synthesis of the functionalized dien backbone **(3)**, it should be possible to prepare either a functionalized form of H_4octaha **(20)** or H_5decaha **(21)**.

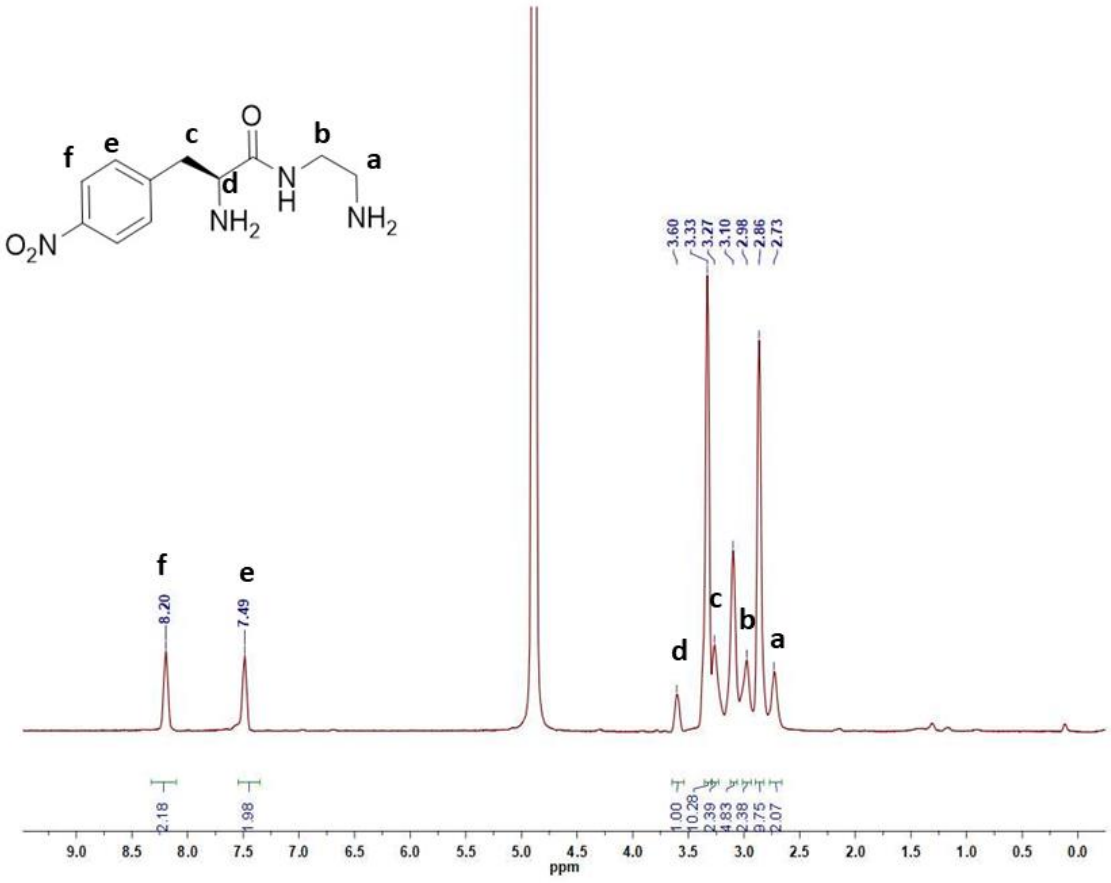

Figure 3-2. ^{1}H NMR spectrum of functionalized diethylenetriamine **4** (400 MHz, CD_3OD, 298 K).

The functionalized dien **(4)** can be used to synthesize functionalized H_4octaha **(20)** using the same conditions for synthesizing H_5decaha **(2)** (*Scheme 3-5*). The amide in

compound **4** will not be alkylated with the addition of the protected hydroxamate arms, solving an issue with the synthesis of H_4octaha **(1)**. In addition to functionalized H_4octaha **(20)**, which functionalizes through a carbon on the backbone, it is possible to functionalize the ligand through a nitrogen atom as in H_4neunpa **(24)**.

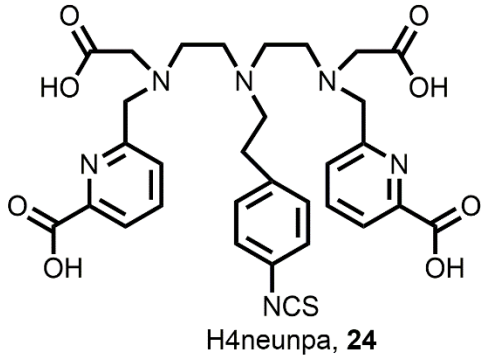

H4neunpa, **24**

Figure 3-3. Bifunctional octadentate ligand, H_4neunpa **(24)**.

The functionalized dien **(4)** can be reduced to an anime **(19)** and used to synthesize functionalized H_5decaha **(21)** incorporating the same reaction conditions for functionalized H_4octaha **(20)** (*Scheme 3-5*). Functionalized H_5decaha **(21)** requires the functionalization to happen at a carbon atom, rather than a nitrogen atom as with H_4neunpa **(24)**, since all nitrogen atoms are fully alkylated by hydroxamate arms. Once purified and characterized by ^{1}H NMR, ^{13}C NMR, and high-resolution mass spectrometry, functionalized H_4octaha **(20)** and functionalized H_5decaha **(21)** can be conjugated to bioconjugates, complexed to metal ions and tested for stability. If the stability is acceptable then functionalized H_4octaha **(20)** and functionalized H_5decaha **(21)** can be used for *in vivo* studies.

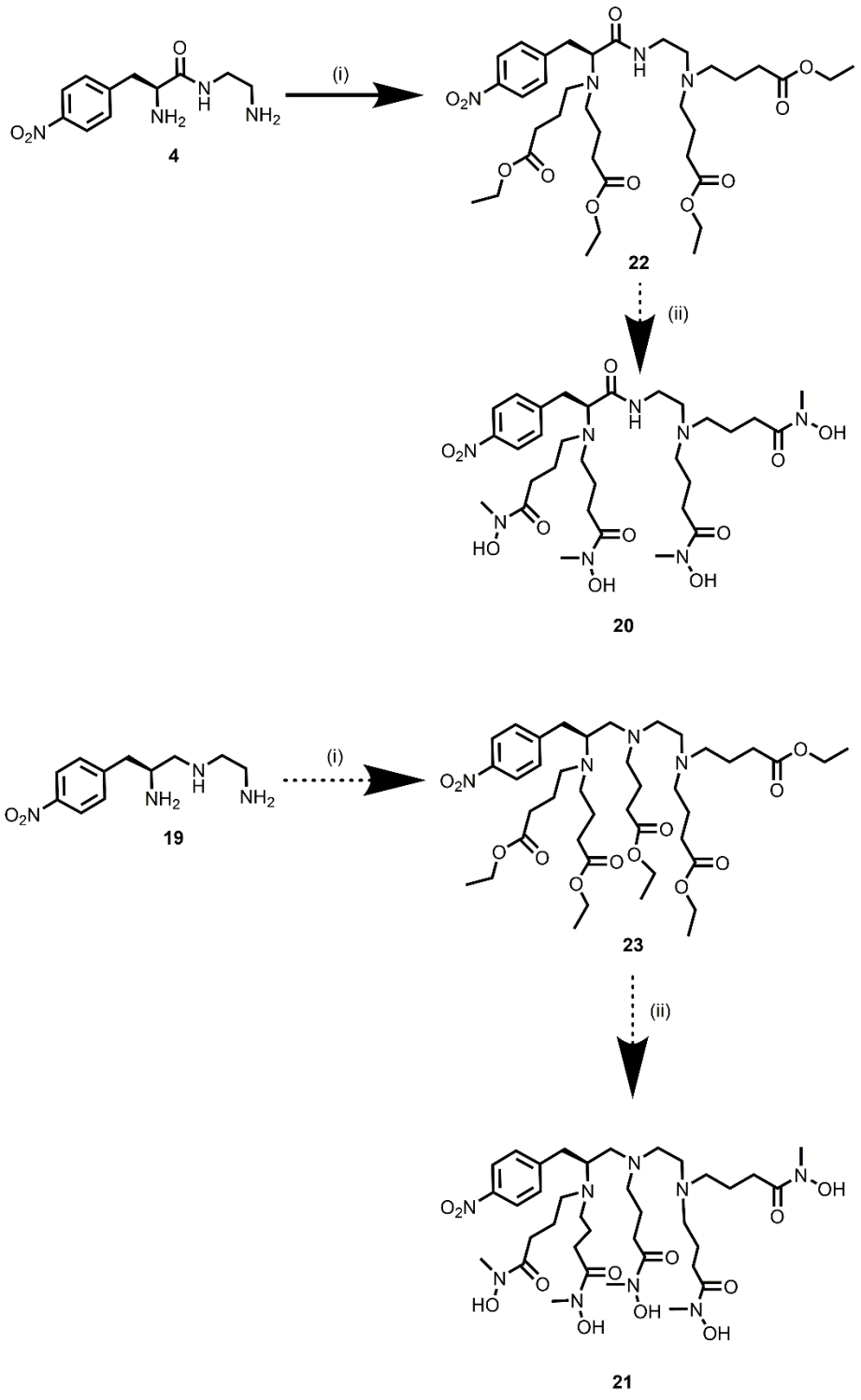

Scheme 3-5. Proposed synthesis of functionalized H_4octaha and H_5decaha. Reagents and conditions: i) $Br(CH_2)_3COOC_2H_5$, K_2CO_3, KI, THF, RT; ii) CH_3NHOH, NaOH, dry MeOH, 298 K.

Chapter 4. Conclusion and Future Directions

4.1 Conclusion

The thesis project focused on the design and synthesis of three hydroxamate-based ligands, H_4octaha **(1)**, H_5decaha **(2)**, and H_4noonha **(3)**, to complex $^{89}Zr^{4+}$ and other hard metal ions. H_4octaha **(1)** synthesis was attempted; however, due to the formation of side products during synthesis of the protected arms and the control of alkylating the dien backbone, the ligand was not completed. The problems led to the development of H_5decaha **(2)**, a decadentate ligand. The synthesis of H_5decaha **(2)** was attempted; however, the yield was too low to perform ^{1}H NMR and ^{13}C NMR analysis. Initial tests with Ga^{3+} complexation support the formation of H_5decaha **(2)** and suggest the ligand complexes with a Ga^{3+} ion and two Na^+ ions. H_4noonha **(3)** makes use of 1,2-bis(aminoethoxylethane) rather than dien as a backbone to allow for full alkylation making an octadentate ligand. While the synthesis of H_4noonha **(3)** was confirmed by ^{1}H NMR, the sample was contaminated. The synthesis was performed again several times and optimized; however, all addition attempts resulted in a yield too low for analysis. The functionalized dien backbone **(4)** was developed to functionalize H_4octaha **(1)** and H_5decaha **(2)**. Compound **4** was easily synthesized to create a dien backbone with a para-nitro phenyl group. The amide group in compound **4** allows four arms to be attached creating functionalized H_4octaha **(20)** and if the amide is reduced before alkylation then functionalized H_5decaha **(21)** can be synthesized. While the synthesis of **4** was successful, the purification proved to be difficult. Reduced pressure and column

chromatography were attempted with limited success in purification. The backbone was purified by precipitation as a HCl salt; however, the insolubility of the salt made analysis difficult.

4.2 Future Work

The synthesis of three, new hydroxamate-based ligand has been progressing with difficulties. The synthesis of the decadentate ligand, H_5decaha **(2)**, is close to completion; however, the purification method still requires improvement and the purified ligand requires further analysis. Currently the separation of five hydroxamates from four hydroxamates by semi-prep HPLC must be further optimized to get a high enough yield for ^{1}H NMR, ^{13}C NMR analysis, and high-resolution mass spectrometry. Once analyzed H_5decaha **(2)** will be tested with numerous different metal ions for complexation, including Zr^{4+}, Ti^{4+}, and Sc^{3+}. The potentially octadentate ligand, H_4noonha **(3)**, was synthesized but due to a contamination the analysis, was not completed. The purification by semi-prep HPLC needs to be further optimized to better separate H_4noonha **(3)** from a three hydroxamate ligand with one ethyl ester group. After optimization and obtaining enough product, ^{1}H NMR, ^{13}C NMR, and high-resolution mass spectrometry can be performed to characterize the ligand. Once analyzed, H_4noonha **(3)** will be complexed with the same metal ions as H_5decaha **(2)**, Zr^{4+}, Ti^{4+}, and Sc^{3+}. While the ligands were designed for complexation with Zr^{4+}, both Ti^{4+} and Sc^{3+} have similar properties to Zr^{4+} making them possible metal ions for complexation and both have β^{+}-emitting isotopes.

Another metal ion to be tested is La^{3+}, to act as a model for the lanthanide series Ln^{3+} and Ac^{3+}. If possible, crystal structures of the complexes will be obtained. After completing the non-radioactive chemistry, the radionuclides $^{89}Zr^{4+}$, $^{44}Sc^{3+}$, $^{45}Ti^{4+}$, $^{132}La^{3+}$, and $^{225}Ac^{3+}$ will be complexed with H_5decaha **(2)** and H_4noonha **(3)** to determine the radiochemical yield and test the *in vitro* stability.

The functionalized dien backbone **(4)** was synthesized but requires further purification before it can be used for functionalized H_4octaha **(20)** and functionalized H_5decaha **(21)**. Once the backbone has been purified and the functionalized ligands characterized, the ligand can be conjugated to a directing vector, complexed to a metal ion, and the stability can be tested. If the stability of the complex is acceptable then the *in vivo* studies can proceed.

References

1) Kostelnik, T. I.; Orvig, C. Radioactive Main Group and Rare Earth Metals for Imaging and Therapy. *Chem. Rev.* **2019,** 119, 902-956.
2) Ramogida, C. F.; Boros, E.; Tarick, B. O.; Zeisler, S. K.; Kumlin, J.; Adam, M. J.; Schaffer, P.; Orvig, C. Evaluation of H_2CHXdedpa, H_2dedpa- and H_2CHXdedpa-N,N'-propyl-2-NI Ligands for ^{64}Cu(II) Radiopharmaceuticals. *Dalton Trans.* **2016,** 45, 13082-13090.
3) Price, E. W.; Zeglis, B. M.; Cawthray, J. F.; Lewis, J. S.; Adam, M. J.; Orvig, C. What a Difference a Carbon Makes: H_4octapa vs H_4C3octapa, Ligands for In-111 and Lu-177 Radiochemistry. *Inorg. Chem.* **2014,** 53, 10412-10431.
4) Saha, G. B. *Fundamentals of Nuclear Pharmacy*. 6th ed.; Springer: New York, N.Y., 2010.
5) Ramogida, C. F.; Orvig, C. Tumour Targeting with Radiometals for Diagnosis and Therapy. *Chem. Commun.* **2013,** 49, 4720-4739.
6) Rahmim, A.; Zaidi, H. PET versus SPECT: Strengths, Limitations and Challenges. *Nucl. Med. Commun.* **2008,** 29, 193-207.
7) Boros, E.; Packard, A. B. Radioactive Transition Metals for Imaging and Therapy. *Chem. Rev.* **2019,** 119, 870-901.
8) Deri, M. A.; Zeglis, B. M.; Francesconi, L. C.; Lewis, J. S. PET Imaging with ^{89}Zr: From Radiochemistry to the Clinic. *Nucl, Med. Biol.* **2013,** 40, 3-14.
9) Liu, S. Bifunctional Coupling Agents for Radiolabeling of Biomolecules and Target-specific Delivery of Metallic Radionuclides. *Adv. Drug. Deliv. Rev.* **2008,** 60, 1347-1370.
10) McInnes, L. E.; Rudd, S. E.; Donnelly, P. S. Copper, Gallium and Zirconium Positron Emission Tomography Imaging Agents: The Importance of Metal Ion Speciation. *Coord. Chem. Rev.* **2017,** 352, 449-516.
11) Vugts, D. J.; Dongen, G. ^{89}Zr-labeled Compounds for PET Imaging Guided Personalized Therapy. *Drug Discov. Today.* **2012,** 8, 53-61.
12) Guerard, F.; Beyler, M.; Lee, Y. S.; Tripier, R.; Gestin, J. F.; Brechbiel, M. W. Investigation of Complexation of ^{nat}Zr(IV) and ^{89}Zr(IV) by Hydroxypyridinones for the Development of Chelators for PET Imaging Applications. *Dalton Trans.* **2017,** 46, 4749-4758.
13) Patra, M.; Bauman, A.; Mari, C.; Fischer, C. A.; Blacque, O.; Haussinger, D.; Gasser, G.; Mindt, T. L. An Octadentate Bifunctional Chelating Agent for the Development of Stable Zirconium-89 Based Molecular Imaging Probes. *Chem. Commun.* **2014,** 50, 11523-11525.
14) Vugts, D. J.; Klaver, C.; Sewing, C.; Poot, A. J.; Adamzek, K.; Huegli, S.; Mari, C; Visser, G.W. M.; Valverde, I. E.; Gasser, G.; Mindt, T. L.; van Dongen, G. Comparison of the Octadentate Bifunctional Chelator DFO*-pPHe-NCS and the

Clinically Used Hexadentate Bifunctional Chelator DFO-pPhe-NCS for ^{898}Zr-immuno-PET. *Eur. J. Nucl. Med. Mol. Imaging.* **2017,** 44, 286-295.

15) Zhai, C.; Summer, D.; Rangger, C.; Franssen, G. M.; Laverman, P.; Haas, H.; Petrik, M.; Haubner, R.; Decristoforo, C. Novel Bifunctional Cyclic Chelator for ^{89}Zr Labeling-Radiolabeling and Targeting Properties of RGD Conjugates. *Mol. Pharm.* **2015,** 12, 2142-2150.
16) Rousseau, J.; Zhang, Z.; Dias, G. M.; Zhang, C.; Colpo, N.; Benard, F.; Lin, K. Design, Synthesis and Evaluation of Novel Bifunctional Tetrahydroxamate Chelators for PET Imaging of ^{89}Zr-Labeled Antibodies. *Bioorg. Med. Chem. Lett.* **2017,** 27, 708-712.
17) Zhai, C.; Summer, D.; Rangger, C.; Haas, H.; Haubner, R.; Decristoforo, C. Fusarinine C, a Novel Siderophore-based Bifunctional Chelator for Radiolabeling with Gallium-68. *J. Label. Compd. Radiopharm.* **2015,** 58, 209-214.
18) Deri, M. A.; Ponnala, S.; Kozlowski, P.; Burton-Pye, B. P.; Cicek, H. T.; Hu, C.; Lewis, J. S.; Francesconi, L. C. p-SCN-Bn-HOPO: A Superior Bifunctional Chelator for ^{89}Zr ImmunoPET. *Bioconjug. Chem.* **2015,** 58, 209-214.
19) Deri, M. A.; Ponnala, S.; Zeglis, B. M.; Pohl, G.; Dannenberg, J. J.; Lewis, J. S.; Francesconi, L. C. Alternative Chelator for ^{89}Zr Radiopharmaceuticals: Radiolabeling and Evaluation of 3,4,3-(LI-1,2-HOPO). *J. Med. Chem.* **2014,** 57, 4849-4860.
20) Buchwalder, C.; Rodriguez-Rodriguez, C.; Schaffer, P.; Karagiozov, S. K.; Saatchi, K.; Hafeli, U. O. A New Tetrapodal 3-Hydroxy-4-Pyridinone Ligand for Complexation of ^{89}Zirconium for Positron Emission Tomography (PET) Imaging. *Dalton Trans.* **2017,** 46, 9654-9663.
21) Spreckelmeyer, S. Metallodrugs for Therapy and Imaging: Investigation of their Mechanism of Action. Ph.D. Dissertation, University of Groningen, Groningen, Netherlands, and University of British Columbia, Vancouver, BC, 2018.
22) Carrasco, M. R.; Brown, R. T.; Serafimova, I. M.; Silva, O. Synthesis of N-Fmoc-O-(N'-Boc-N'-methyl_aminohomoserine, and Amino Acid for the Facile Preparation of Neoglycopeptides. *J. Org. Chem.* **2003,** 68, 195-197.
23) Gudmundsdottir, A. V.; Paul, C. E.; Nitz, M. Stability Studies of Hydrazide and Hydroxylamine-based Glycoconjugates in Aqueous Solution. *Carbohydr. Res.* **2009,** 334, 278-284.
24) Wharton, L. Chemistry Department, University of British Columbia, BC. Personal Communication, 2017-2018.
25) Wang, X. Chemistry Department, University of British Columbia, BC. Personal Communication, 2017-2019.
26) Reddy, D. N.; Ballante, F.; Chuang, T.; Pirolli, A.; Marrocco, B.; Marshall, G. R. Design and Synthesis of Simplified Largazole Analogues as Isoform-selective Human Lysine Deacetylase Inhibitors. *J. Med. Chem.* **2016,** 59, 1613-1633.

27) Brechbiel, M. W.; Gansow, O. A.; Atcher, R. W.; Schlom, J.; Esteban, J.; Simpson, D. E.; Colcher, D. Synthesis of 1-(p-Isothiocyanatobenzyl) Derivatives of DTPA and EDTA. Antibody Labeling and Tumor-Imaging Studies. *Inorg. Chem.* **1986,** 25, 2772-2781.

Appendix

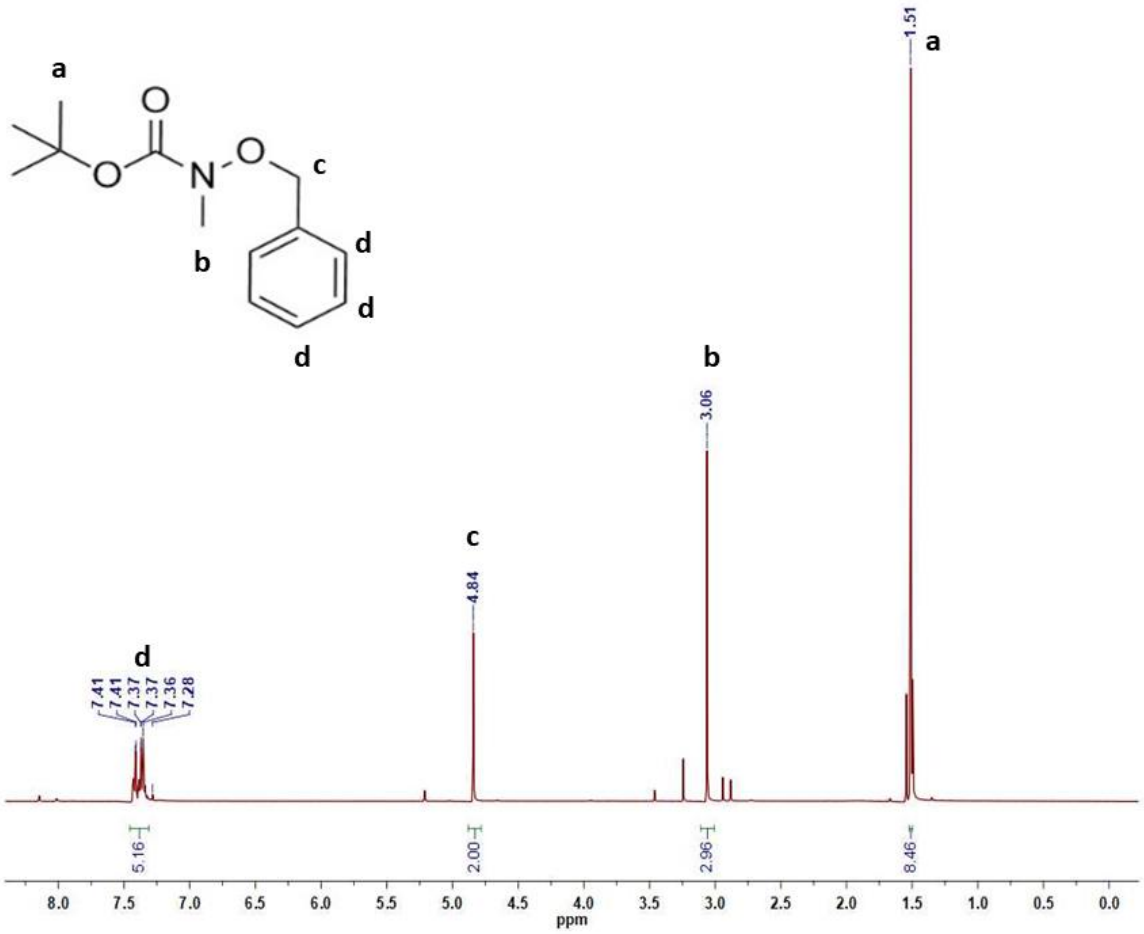

Figure A-1. ^{1}H NMR spectrum of **13** (400 MHz, $CDCl_3$, 298 K).

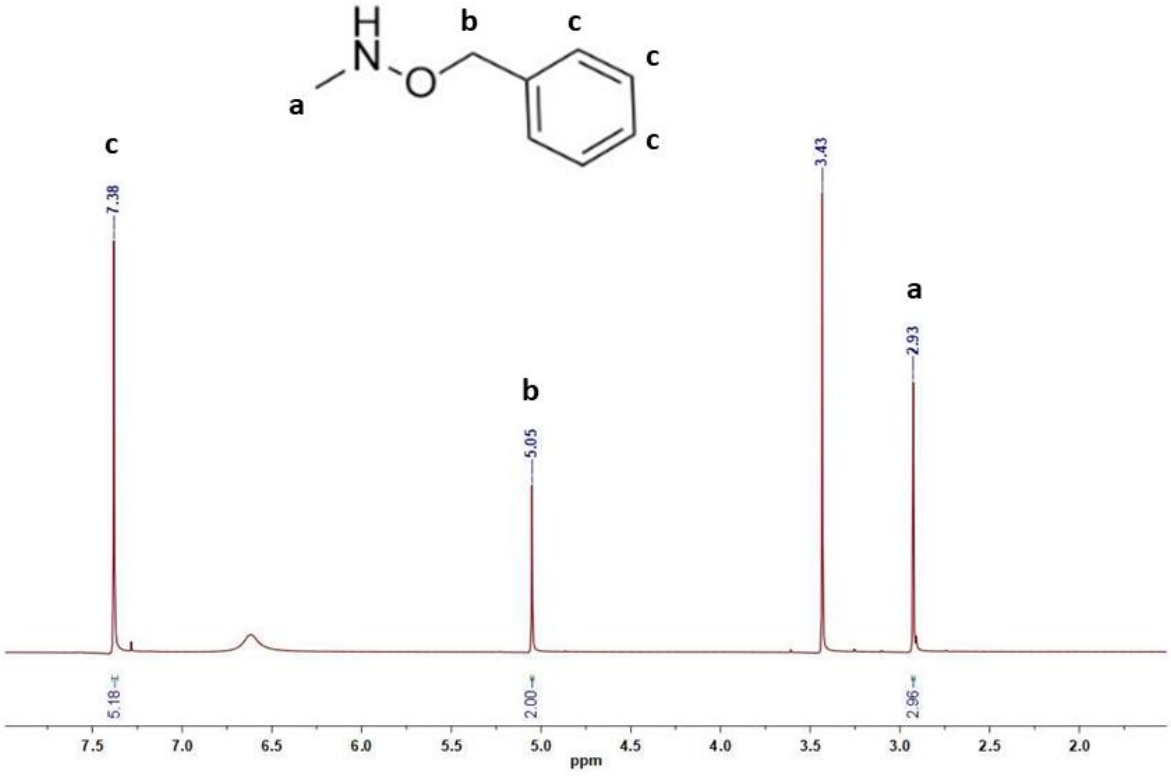

Figure A-2. ^{1}H NMR spectrum of **14** (400 MHz, CD_3OD, 298 K).

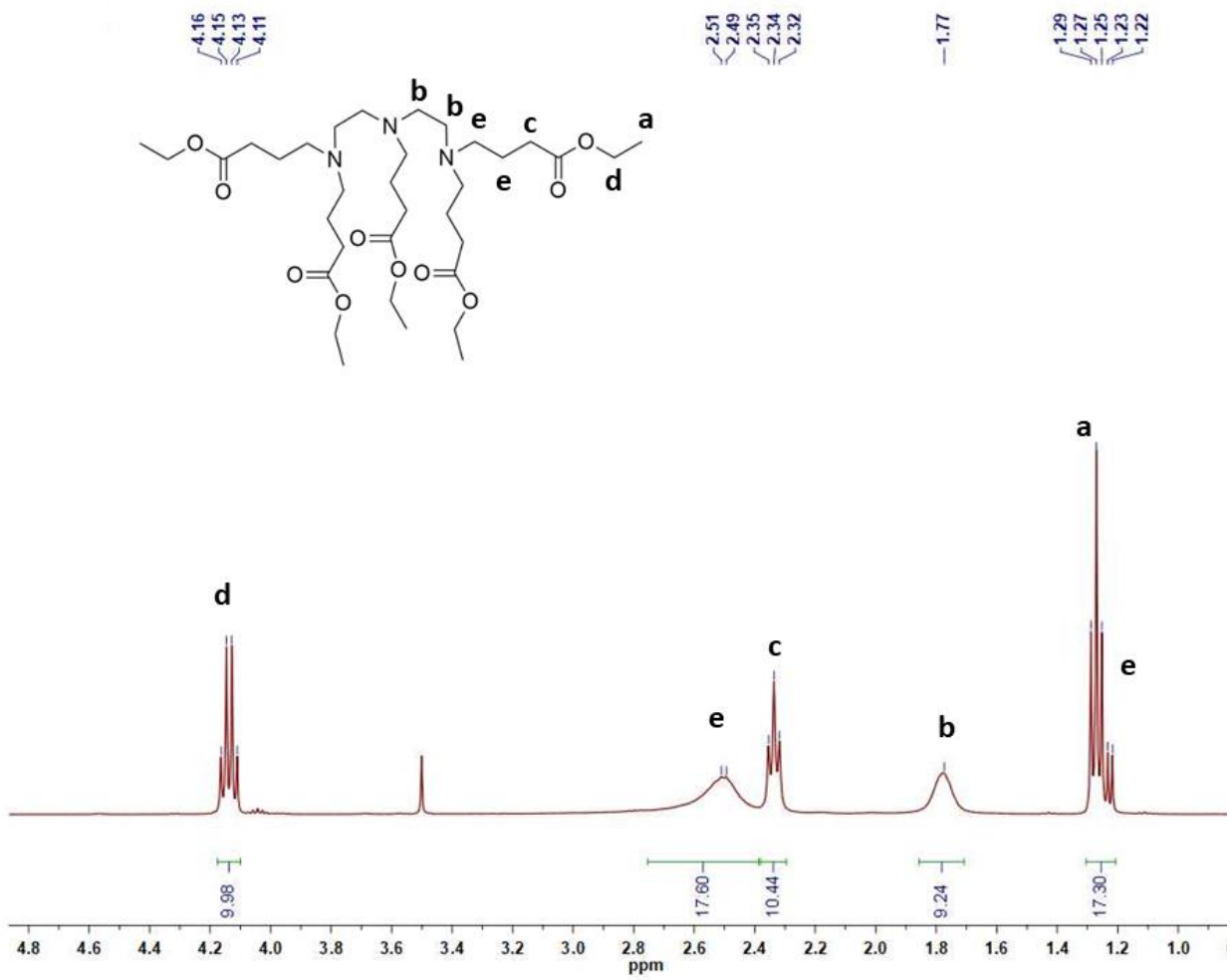

Figure A-3. ^{1}H NMR spectrum of **16** (400 MHz, $CDCl_3$, 298 K).

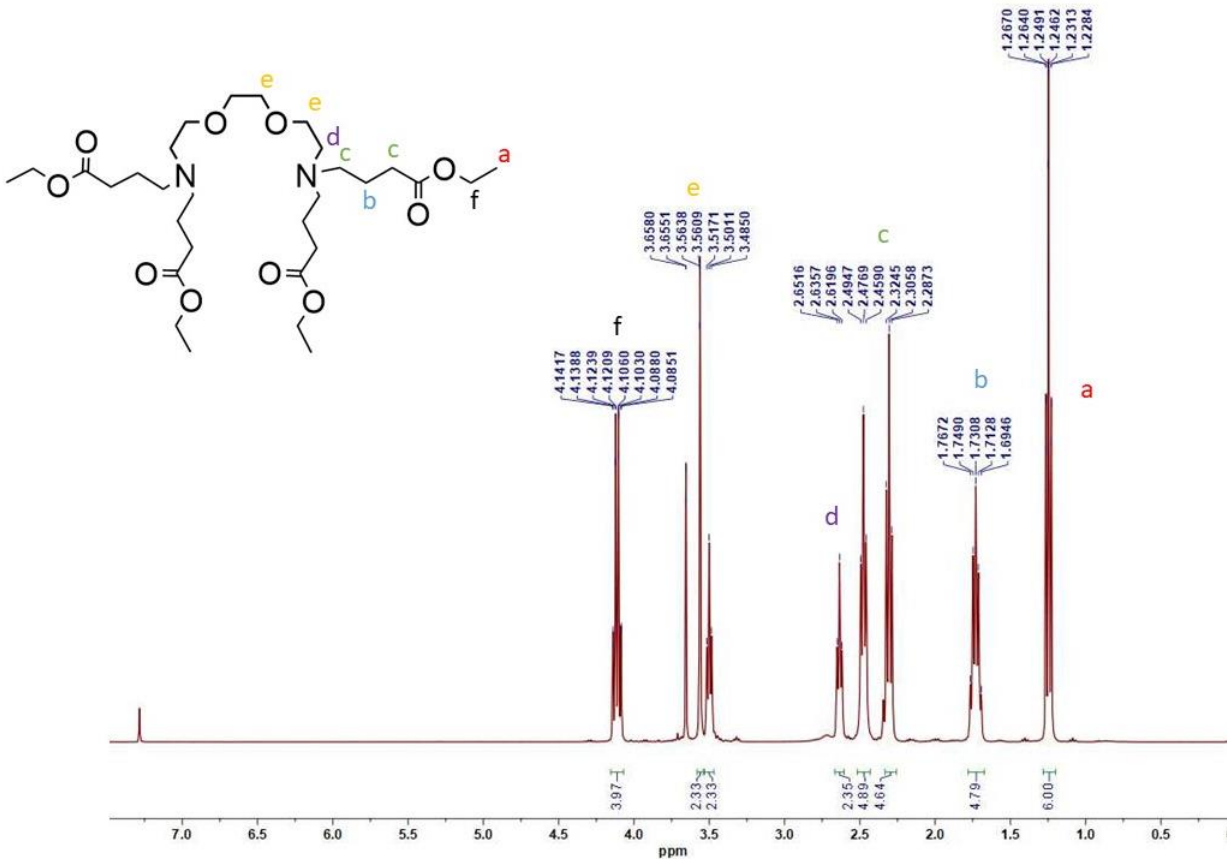

Figure A-4. ^{1}H NMR spectrum of compound **17** (400 MHz, $CDCl_3$, 298 K).

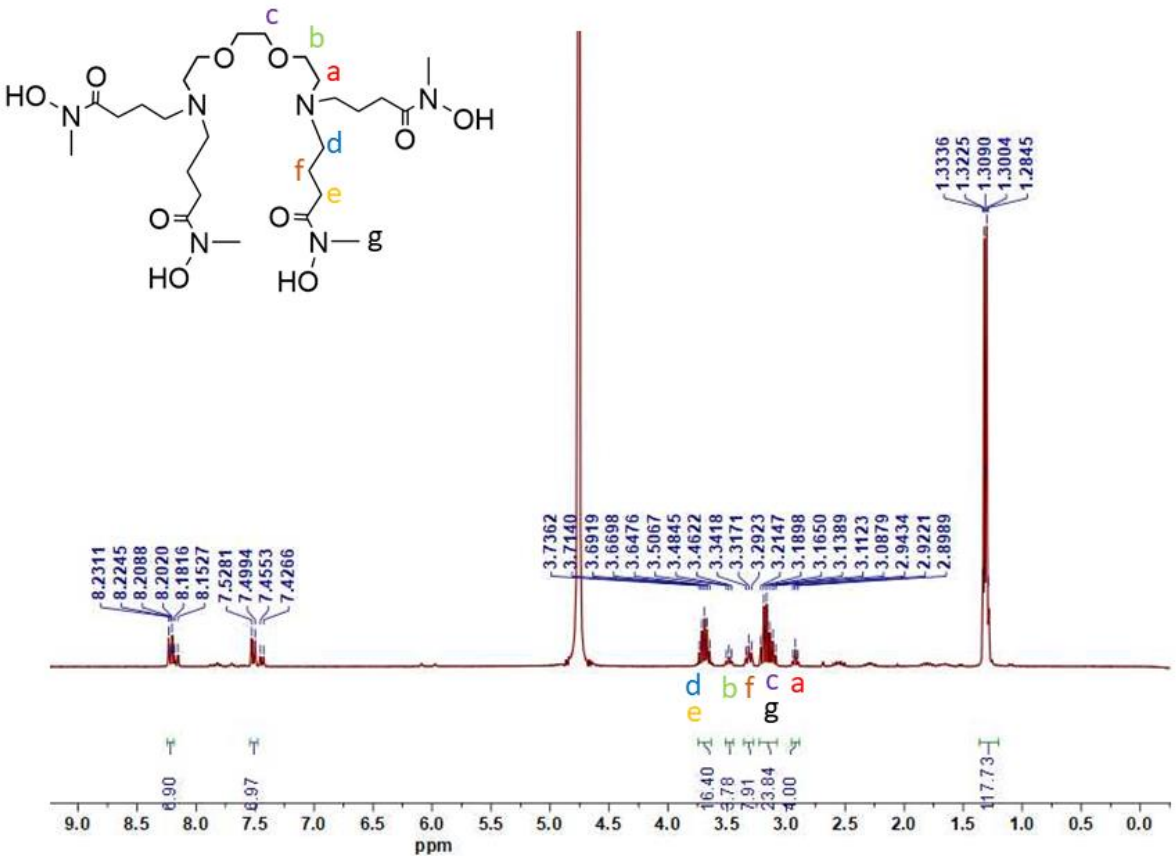

Figure A-5. ^{1}H NMR spectrum of H_4noonha (300 MHz, D_2O, 298 K).